2016

Using Fluorescence to Characterize Four Day Simulated Distribution System Trihalomethane Content in Florida Groundwaters

Jonathan Ousley
University of Central Florida

USING FLUORESCENCE TO CHARACTERIZE FOUR DAY SIMULATED DISTRIBUTION SYSTEM TRIHALOMETHANE CONTENT IN FLORIDA GROUNDWATERS

by

JONATHAN T. OUSLEY
B.S. University of Central Florida, 2015

A thesis submitted in partial fulfillment of the requirements
for the degree of Master of Science
in the Department of Civil, Environmental, and Construction Engineering
in the College of Engineering and Computer Science
at the University of Central Florida
Orlando, Florida

Fall Term
2016

Major Professor: Steven J. Duranceau

ABSTRACT

The United States Environmental Protection Agency (USEPA) regulates public water systems and has established limits for certain disinfection by products (DBPs) that have been linked to health effects, such as bladder cancer. The regulation of DBPs, specifically total trihalomethanes (TTHMs) and haloacetic acids (HAAs), have encouraged water treatment professionals to assess the type and amount of organic precursors in their supplies. Three of the more common water quality parameters that are monitored as DBP surrogates include dissolved organic carbon (DOC), ultraviolet absorbance (UV_{254}), and specific ultraviolet absorbance (SUVA). Although DOC, UV_{254}, and SUVA have been effectively correlated to DBP formation, efforts to correlate fluorescence excitation emission matrices (FEEM) to DBP formation remains limited within the drinking water community. In this research, a fluorescence regional integration (FRI) approach was used to compare FEEM with DOC, UV_{254}, and SUVA as an alternative surrogate for characterizing TTHMs for groundwater sources located in south central Florida.

To quantitatively evaluate FEEM, DOC, UV_{254}, and SUVA as TTHM precursor surrogate parameters, a statistical correlation analysis was employed. Thirteen groundwater samples were collected from various Central Florida groundwater wells in Lake County, Polk County, and Palm Beach County, and analyzed for FEEM, DOC, UV_{254}, and SUVA prior to determining the four-day TTHM concentration using a simulated distribution system dosing procedure. The FRI method was then used to quantify FEEM by dividing the three-dimensional matrix into five distinct regions, each representing a unique organic constituent. The volume under each region was determined and used for the correlation analysis.

It was determined that a combinations of regions III and V of the FEEM possessed a strong linear correlation to four day TTHM content (R^2 = 0.95) as compared to DOC (R^2 = 0.906), UV_{254} (R^2= 0.84), SUVA (R^2 = 0.640), and the individual regions of the FEEM. However, DOC showed the strongest correlation when a second order polynomial regression was used (R^2 = 0.937). Results for the individual regions of the FEEM revealed four day simulated TTHM correlation coefficients of 0.25, 0.62, 0.86, 0.74, and 0.88 for regions I through V respectively. These values indicated that a combination of regions III and V, which represent the fulvic and humic-like organic fractions detected by FEEM respectively, was the most accurate four day simulated TTHM precursor surrogate parameter based on the groundwater supplies tested. These results reveal that although DOC is still one of the strongest surrogate parameters to TTHM formation, fluorescence has also shown to also be a potentially strong surrogate for groundwaters. The implications of these results signify that fluorescence monitoring could be a viable method of measuring organic content in groundwaters once the technology further develops.

This thesis is dedicated to my parents: Landon and Theresa Ousley. Thank you for your continuous love and support.

ACKNOWLEDGMENTS

The work conducted on this study would not have made possible without the support of a number of individuals. The author would like first and foremost thank Dr. Steven Duranceau for his guidance serving as the author's committee chair, as well as for being given the opportunity to partake in this research and further the author's educational endeavors. Appreciation would also like to be extended to Dr. Woo Hyoung Lee, and Dr. Anwar Sadmani for serving as committee members and for their time and expertise in reviewing this document. The author would also wish the express gratitude to the efforts of Mrs. Maria Real-Robert, the Civil, Environmental, and Construction Engineering laboratory coordinator for her guidance and assistance. Special thanks is given to Paul Biscardi and David Yonge for their continuous mentoring and guidance as well as to Ari Hadar for his additional support in lab and data analyses. The author further wishes to express gratitude for the contributions and assistance of UCF students Benjamin Yoakum, Angela Rodriguez, Samantha Meyers, Carlyn Higgins, Martin Coleman, Jessica Cormier, Maria Arenas, Cassidy Conover, Hadi Toure, and Ana Rosabel. The author would also like to sincerely thank the operational staff for the water treatment facilities at the Polk County, Lake County, and Town of Jupiter locations for their assistance and coordination during sampling events.

TABLE OF CONTENTS

LIST OF FIGURES

LIST OF TABLES

LIST OF ABBREVIATIONS

AMH	Amber Hills Well
AH1	Anderson Hill Well 1
AH2	Anderson Hill Well 2
AU	Arbitrary Units
BP2	Babson Park Water Treatment Facility 2
D/DBP	Disinfectants / Disinfection By-Products
DBPs	Disinfection By-Products
DOC	Dissolved Organic Carbon
EEM	Excitation – Emission Matrix
FEEM	Fluorescence Excitation-Emission Matrix
FRI	Fluorescence Regional Integration
GC	Gas Chromatograph
HAA	Haloacetic Acid
IDSE	Initial Distribution System Evaluation
JUP	Jupiter Water Treatment Facility
LG1	Lake Groves Well 1
LG2	Lake Groves Well 2
LG3	Lake Groves Well 3
LR	Lake Ridge Well
LRAA	Locational Running Annual Average
LWL / LCL	Lower Warning Limit / Control Limit
MRDLG	Maximum Residual Disinfectant Level Goals
MRDL	Maximum Residual Disinfectant Levels
NOM	Natural Organic Matter
NPDOC	Non-Purgeable Dissolved Organic Carbon
NPOC	Non-Purgeable Organic Carbon
OLL	Oranges / Lake Louisa Well
PARAFAC	Parallel Factor Analysis
POE	Point of Entry

POC	Purgeable Organic Carbon
RU	Raman Units
RPD	Relative Percent Difference
RAA	Running Annual Average
SUVA	Specific Ultraviolet Absorbance
TOC	Total Organic Carbon
THMs	Trihalomethanes
TTHMs	Total Trihalomethanes
UV_{254}	Ultraviolet Absorbance at 254 nanometers
USEPA	United States Environmental Protection Agency
UCF	University of Central Florida
UWL / UCL	Upper Warning Limit / Control Limit
V1	Vista Well 1
V2	Vista Well 2
V3	Vista Well 3
WTF	Water Treatment Facility

CHAPTER 1: INTRODUCTION

Disinfection has become a widely used practice in the treatment of potable drinking water in order to protect the public from exposure to pathogenic bacteria and viruses. One major concern with the use of chlorine based disinfectants is that it can react with natural organic matter (NOM) present in source water to form suspected carcinogens which may cause chronic illness over time. These suspected carcinogens have come to be referred to as disinfection by-products (DBPs). Trihalomethanes (THMs) and haloacetic acids (HAAs) are two classes of DBPs regulated by the United States Environmental Protection Agency's (USEPA) Disinfectants and Disinfection By-Product (D/DBP) Rule to limit exposure of the public to these compounds.

In order to comply with these regulations, DBP surrogates, such as dissolved organic carbon (DOC), ultraviolet absorbance (UV_{254}), and specific ultraviolet absorbance (SUVA) are monitored by water purveyors. Although DOC, UV_{254}, and SUVA have been effectively correlated to DBP formation, both parameters only describe a limited fraction of NOM in source waters. Fluorescence spectroscopy is a technology that has received recent attention due to its ability to characterize a larger fraction of NOM than DOC, UV_{254}, and SUVA. Application of fluorescence spectroscopy through the use of fluorescence excitation-emission matrices (FEEMs) in the drinking water industry include tracking NOM through treatment process trains (Baghoth et al., 2011) and identifying organic contribution in membrane fouling (Peiris et al., 2010).

While some uses for fluorescence analysis in the drinking water industry have been explored, efforts to correlate FEEMs to THM formation remains limited to surface waters. One study by Yang and colleagues (2008) assessed the correlation between NOM and DBP formation during

chloramination while utilizing FEEMs in a portion of their research. Results revealed that a weak correlation (R^2=0.42) was shown between a portion of the FEEM and the formation of chloroform, one of the four compounds that make up the total trihalomethane (TTHM) matrix. However, this study was focused on various DBPs including dichloroacetic acid, chloroform, dichloroactonitrile, and total organic halogen (TOX) in surface water, leaving room for further investigation in assessing the correlation of FEEMs to regulated DBPs in groundwaters. Other studies have been conducted to identify the use of fluorescence as an alternative organic analysis for surface waters, however, the application of fluorescence spectroscopy for groundwaters remains limited.

The purpose of this research was to compare FEEMs with DOC, $UV_{254,}$ and SUVA as an alternative surrogate parameter for characterizing TTHMs for groundwater sources in south central Florida. Source water locations included groundwater wells from Lake County, Polk County, and Palm Beach County. A statistical correlation analysis was employed to quantitatively evaluate the use of FEEM, DOC, UV_{254}, and SUVA as four day TTHM precursor surrogate parameters.

CHAPTER 2: LITERATURE REVIEW

The use of disinfectants for the removal of disease-causing organisms in potable drinking water treatment to protect public health and limit exposure to pathogens has been widely used over the past century. The most common disinfection processes involves the addition of chlorine, either in the form of chemical chorine, chlorine dioxide, or chloramines, to inactivate microorganisms and pathogens in drinking water (Richardson, 2005). However, an unintended consequence of the addition of chlorinated compounds is that it acts to oxidize naturally occurring organic matter in the water to form suspected carcinogens referred to as disinfection by-products (DBPs). Long term exposure to DBPs has become a concern to public health and a growing topic of interest for the drinking water community.

Overview of Disinfection By-Product Regulations

The presence of chloroform in finished drinking water led to the identification of the first class of halogenated DBPs known as trihalomethanes (THMs) (Rook, 1974). The carcinogenic risk of the ingestion of chloroform was identified by the National Cancer Institute in 1976 which prompted the USEPA to regulate four THMs (chloroform ($CHCL_3$), bromodichloromethane ($CHBrCl_2$), dibromochloromethane ($CHBr_2Cl$), and bromoform ($CHBr_3$)) in drinking water starting in 1979 (USEPA, 1979).

The promulgation of the Stage 1 Disinfectants D/DBP Rule in 1998 introduced four major changes to previous regulations: 1) The maximum contaminant level (MCL) of THMs was reduced from 100 micrograms per liter (μg/L) to 80 μg/L, 2) five haloacetic acids (HAA_5) were included as regulated contaminants, 3) Chlorite (ClO_2^-) and Bromate (BrO_3^-) were included as regulated

contaminants, and 4) the establishment of maximum residual disinfectant levels (MRDLs) and maximum residual disinfectant level goals (MRDLGs). A summary of the Stage 1 D/DBP Rule is presented in Table 2.1.

Table 2.1: Stage 1 D/DBP Rule Overview (USEPA, 1979)

Disinfection By-Product	MCL (mg/L)	MRDL (mg/L)	MRDLG (mg/L)
Total Trihalomethanes	0.080	4.0 (as Cl_2)	4.0 (as Cl_2)
Chloroform			
Bromodichloromethane			
Dibromochloromethane			
Bromoform			
Total HAA_5	0.060	4.0 (as Cl_2)	4.0 (as Cl_2)
Chloroacetic acid			
Dichloroacetic acid			
Trichloroacetic acid			
Bromoacetic acid			
Dibromoacetic acid			
Bromate	0.010	NA	NA
Chlorite	1.0	0.8 (as ClO_2)	0.8 (as ClO_2)

The four regulated THMs were initially controlled at MCL of 100 µg/L until 1998 when the Stage 1 Disinfectants D/DBP Rule was promulgated to reduce the MCL of THMs to 80 µg/L and include the regulation of five new contaminants called haloacetic acids (HAA_5) (USEPA, 1998). The five HAAs include monochlorocacetic acid, dichloroacetic acid, trichloroacetic acid, monobromoacetic acid, and dibromoacetic acid which together are regulated at a MCL of 60 µg/L. The MCLs for both regulated DBP chemical groups was measured based on a running annual average (RAA), which represented the average over a one-year period of the samples collected in a utility's distribution system. The Stage 1 D/DBP rule also established MRDLs and MRDLGs to limit the amount of DBP formation in the distribution system.

The Stage 2 D/DBP rule was promulgated in January 2006 by the EPA to build upon the foundation laid down by the Stage 1 D/DBP rule to further reduce consumer exposure to DBPs. The Stage 2 D/DBP Rule requires the identification of locations in a drinking water system with the highest potential DBP concentrations through the implementation of an initial distribution system evaluation (IDSE) and evaluate compliance using a locational running annual average (LRAA) (USEPA, 2006).

DBP Formation Chemistry

DBPs are formed as a result of the chemistry that occurs when disinfectants oxidize naturally occurring NOM and inorganic species. NOM, measured as dissolved organic carbon (DOC) or total organic carbon (TOC), represents the organic precursors to DBPs while the bromide ion serves as the inorganic precursor (Amy et al., 2000). Depending on the type of disinfectant used, the reaction changes as well as the reduced end product. The typical disinfectants used are chlorine, ozone, chlorine dioxide, and monochloramines, and each can react differently to form different forms of DBPs (Krasner et al., 1989). In this study, sodium hypochlorite was used to disinfect the collected water samples, and will be the primary focus for the remaining discussion on formation chemistry.

Chlorine, as a disinfectant, is available as gaseous chlorine, liquid sodium hypochlorite (NaOCL), or in powdered form as calcium hypochlorite. Regardless of which form is used, chlorine acts as a strong oxidizing agent and often is consumed rapidly in side reactions such that excessive amounts are required to provide adequate disinfection. The primary reducing agents that react with the chlorine are hydrogen sulfide, manganese (II), iron (II), sulfite, bromide, and nitrite. These

constituents rapidly consume chlorine and reduce the chlorine available to react with organic matter to form DBPs (Amy et al., 2000).

The primary fraction of the NOM that reacts with the chlorine to form DBPs has been identified as humic and fulvic acids. These two organic constituents are shown to have high reactivity with chlorine due to their high levels of aromaticity (Singer, 1999). Aromaticity, a descriptor used for stable carbon ring molecules, has historically been measured in drinking water using specific ultraviolet absorbance (SUVA) (Hua et al., 2015). SUVA is defined as the ratio of ultraviolet absorbance at 254 nm (UV_{254}) to the DOC content of a water sample. This parameter has been shown to have a strong correlation with TTHM and HAA formation (Jung et al., 2008) due to aromatic humic substances exhibiting higher UV_{254} measurements than aliphatic and non-humic substances (Weishaar et al., 2003).

Chloroform, one of the most dominant THMs, is often formed through a series of oxidation and substitution reactions with functional groups of humic substances. The presence of bromide in water can also react with NOM to form hypobromous acid as well as brominated compounds such as bromoform. The remaining two regulated THMs ($CHBrCl_2$ and $CHBr_2Cl$) are formed in the presence of both chlorine and bromide forming bromochlorinated compounds.

A number of factors influence the aforementioned reactions. Amy and colleagues (2000) showed that contact time, temperature, pH, and the concentration of both the precursor and disinfectant are some of the primary variables that influence the formation of DBPs. It has been shown that an increase in contact time, temperature, or concentration as well as a high pH, will increase the rate at which DBPs are formed (Zhang et al., 2013).

Analysis of DBP Precursors

As previously mentioned, NOM is the primary precursor to DBP formation along with certain inorganic components of the water such as bromide. The ability to efficiently and cost-effectively analyze precursor materials could aid in developing a more complete understanding of DBP formation for a particular disinfected water. This section will outline the different techniques commonly used to analyze organic precursors as well as describe their advantages and disadvantages.

Dissolved Organic Carbon

Total organic carbon (TOC) is a measurement of the organic content of a water sample that measures the total amount of carbon atoms that are covalently bonded in organic molecules (American Public Health et al., 2005). Dissolved organic carbon (DOC) is a subset of the TOC that represents the fraction that passes through a 0.45 micrometer (μm) filter. This accounts for the particulate fraction that is typically removed prior to the disinfection process for most water treatment facilities, and is therefore an appropriate parameter for determining the organic content that has the ability to react with the disinfectant to form DBPs.

The preferred method of analysis for determining TOC or DOC for drinking water samples is a non-purgeable organic carbon (NPOC) method (Wallace et al., 2002). This method involves the introduction of a small amount of inorganic acid to an inorganic carbon removal chamber. The process of acidification of the sample converts the inorganic carbon to carbonic acid which is often gas-stripped to remove it from the sample. The volatile fraction of the organic content is referred to as purgeable organic carbon (POC) which is often negligible for most drinking waters. In these cases, the NPOC is determined to be equivalent to the TOC. The gas stripping process often

removes the POC from the sample resulting in the ability to determine the NPOC from what remains (Wallace et al., 2002).

DOC has historically been acknowledged as a strong surrogate parameter for DBP formation. However, the use of using DOC measurements to have a better understanding THM formation potential was eventually substituted with ultraviolet absorbance analysis as it was a faster and more cost efficient method compared to DOC analysis.

Ultraviolet Absorbance

Ultraviolet absorbance at a wavelength of 254 nanometers (UV_{254}) is often used as a measure of the organic content for a sample of water. By passing light through a sample, a portion of that light is either absorbed or scattered by the presence of particulate or dissolved organic matter in the sample. The wavelength of the incident light is set at 254 nm to specifically target organic matter, with high aromaticity that will absorb ultraviolet light at this wavelength allowing for the determination of the organic matter in a given water sample (Amy et al., 2000).

As previously discussed, humic acids represent a fraction of NOM in drinking water sources which has been shown to be highly reactive with disinfectants like chlorine to form DBPs. Humic acids are naturally highly aromatic and larger in molecular weight as well as size when compared to other fractions of organic matter. Due to UV_{254} measurements being able to detect organics with higher aromatic properties, it is an appropriate analysis for waters with organics that contain humic acids. This theoretically makes UV_{254} measurements an ideal indicator of a water's potential to form DBPs upon chlorine addition. The relatively rapid, low cost of analysis has led UV_{254}

measurements to overshadow the use of TOC or DOC measurements to determine DBP formation potential.

Specific Ultraviolet Absorbance (SUVA)

SUVA is calculated by normalizing the UV_{254} to DOC and is recorded in units $mg \cdot m^{-1} \cdot L^{-1}$. SUVA measures the average absorptivity of the DOC in a water sample and has historically been used as a surrogate parameter for DOC aromaticity (Weishaar et al., 2003). As discussed previously, humic and fulvic acids are highly aromatic; this has led to the use of SUVA as an alternative surrogate parameter for TTHM formation similar to UV_{254}.

SUVA has been shown to have a strong linear correlation to TTHM formation for SUVA values ranging from 1 to 3 L/mg/m. However, the correlation has been shown to be much weaker for SUVA values below 1.0 L/mg/m (Ates et al., 2007) as well as for values above 3.0 L/mg/m (Weishaar et al., 2003). The results from these studies indicate that SUVA is a conditional parameter, useful for certain waters that fall in average SUVA ranges but not for the upper and lower ends.

Fluorescence Spectroscopy

Fluorescence spectroscopy, similar to UV_{254}, measures the ability of organics in a sample of water to absorb incident light and fluoresce resulting in a change in wavelength of the light (Bridgeman et al., 2011). However, UV_{254} measures only wavelength while fluorescence spectroscopy scans a range of wavelengths using a range of indecent light wavelengths. The molecular chemistry involved in this phenomena are such that electrons become excited as the molecule absorbs light, raising it from the neutral ground state to a higher, unoccupied orbital. This is known as excitation

and can occur over a wide range of orbital states, often creating broad band peaks (C. A. Stedmon et al., 2003). After excitation has been achieved, the molecule can no longer sustain the energy required to maintain at the higher orbital level and eventually drops down to the ground state. This causes a release of a wavelength of light that is less than that of the excitation wavelength due to energy loss. This release of light is called the emission wavelength and the process of analyzing fluorescence involves the measurement of the intensity of the light from the incident excitation wavelength to the received emission wavelength (C. A. Stedmon et al., 2003).

The analysis of a sample using fluorescence spectroscopy yields a three dimensional graph that plots excitation and emission on the x and y axis, and the intensity on the z axis and is referred to as an excitation-emission matrix (EEM). Different fluorophores and fluorescing substances fluoresce at different excitation – emission combinations resulting in various peaks that appear in different regions of the EEM. The EEM, however, contains a large amount of information, and methods of data analysis for these plots have been limited (Chen et al., 2003). This has resulted in a number of techniques that have been developed over the last decade that utilize different approaches to analyze the data provided in the EEMs. Methods such as peak-picking (Korak et al., 2014), parallel factor analysis (PARAFAC) (Murphy et al., 2013), and fluorescence regional integration (FRI) (Chen et al., 2003) will be discussed in further detail herein.

Peak Picking Method

The peak picking method was the original technique used for quantitative fluorescence analysis of EEMs (Korak et al., 2014). The concept behind the method was that for a variety of water samples, peaks would appear on the EEM at specific excitation-emission combinations and those peaks were representative of a particular organic substance (humic, fulvic, protein-like, etc.). Three

major peaks were defined as follows: 1) peak A - humic-like substances stimulated by UV excitation, 2) peak C - humic-like substances stimulated by visible excitation, and 3) peak T – tryptophan and protein-like material related to biological activity (Coble, 1996). These three peaks and their locations are shown on an example EEM in Figure 2.1.

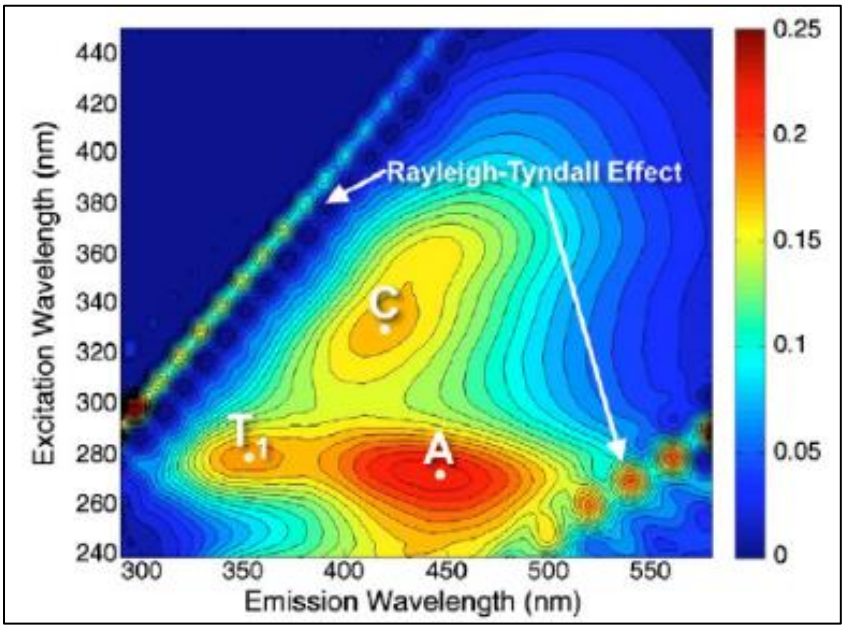

Figure 2.1 Standard Peaks for Peak Picking Method (adapted from (Hickenbottom et al., 2013))

While this method served as a way to analyze quantitative data from an EEM, it ignored a large portion of the data set. This led to the development of more advanced analysis techniques that aimed to utilize a larger portion of the data set to determine more accurate characterization of the fluorescing organics material.

Parallel Factor Analysis (PARAFAC)

PARAFC analysis is multivariate data analysis technique designed to overcome the limitations of alternative EEM analysis techniques (Murphy et al., 2013). The PARAFAC analysis decomposes

the fluorescence signal into individual, underlying fluorophores for a particular data set of large sample size. This is done through the use of a multi-way (three-way) analysis to describe the three dimensions of the EEM: excitation, emission, and intensity. Equation 2-1 is used as the foundation of the PARAFAC model as adapted from Stedmon et al (2008):

$$\boldsymbol{x_{ijk}} = \sum_{\boldsymbol{f=1}}^{\boldsymbol{F}} \boldsymbol{a_{if} b_{jf} c_{kf}} + \boldsymbol{\varepsilon_{ijk}}\ , \boldsymbol{i} = \mathbf{1},..,\boldsymbol{I}; \boldsymbol{j} = \mathbf{1},..,\boldsymbol{J}; \boldsymbol{k} = \mathbf{1},..,\boldsymbol{K}; \qquad (2\text{-}1)$$

In Equation 2-1, x^{ijk} is the fluorescence intensity of sample *i* measured at emission wavelength *j* and excitation wavelength *k*. Residual noise and interference is represented in the final term ε_{ijk}. The result of the model are the paramters *a*, *b*, and *c*, which represent the concentration, emission spectra, and excitation spectra of the underlying fluorophores (C. Stedmon et al., 2008). Figure 2.2 is a visual representation of Equation 2-1 and depicts the three-dimensional multi-way analysis of the data.

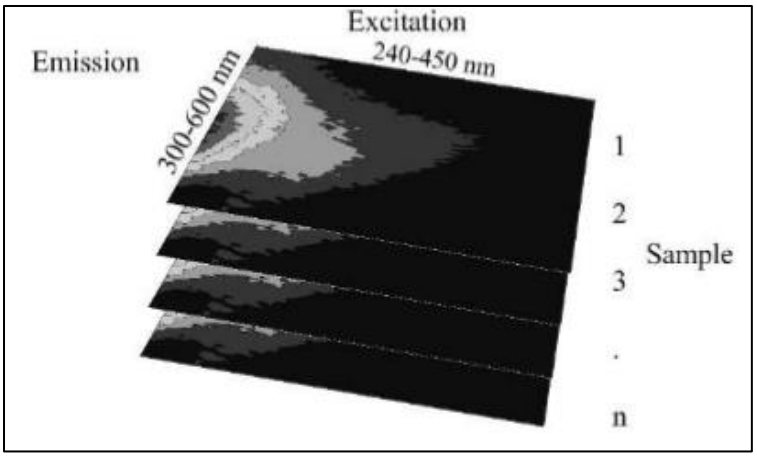

Figure 2.2 Visual Model for PARAFAC Analysis adapted from (C. Stedmon et al., 2008)

The number of samples needed to obtain an adequate PARAFAC model is arbitrary and depends on the nature of the sample water and the focus of the study. Generally, it is shown that the modeling processes is simplified with a larger sample set as the number of common factors between samples become fewer and easier to identify. However, it is recommended that data sets range from approximately 20 – 100 samples (C. Stedmon et al., 2008). The nature of the sample also needs to be taken into consideration as a wide variety of samples may result in a less accurate model for a given particular study. This being taken into consideration, PARAFAC models are often used to characterize specific sets of data for a location or specific quality of water and are not appropriate to be used universally.

The number of factors determined through the PARAFAC model is also variable depending on the data set and its determination is often an iterative process. The core consistency of the model is checked as the number of factors assessed increases. When there large drop in core consistency between a model of n parameters and a model of $n+1$ parameters occurs, the number of factors used in the model is recommended to be the value of n. Each of these factors is representative of an influential organic component and its origin such as humic acids of marine origin or tyrosine introduced into estuarine water via microbial activity (Hall et al., 2007). While some of these factors have been shown to be consistent across multiple PARAFAC analysis using different samples, it has yet to be shown that these factors are universal.

Although PARAFAC models are one of the most comprehensive methods for EEM analysis, their limitations to site specificity and large required data set made it an inappropriate analysis technique for the research presented herein.

Fluorescence Regional Integration (FRI)

Fluorescence regional integration is a quantitative method that utilizes the full range of the EEM spectrum. The method delineates an EEM into five regions based on organic characteristics and historical data and the integration of the volume beneath each region is determined to quantify the organic makeup of a water sample (Chen et al., 2003). The range of the excitation emission spectra is bounded such that excitation wavelengths are read from 200 to 400 nanometers (nm) in 5 nm increments while emission wavelengths are read from 280 to 600 nm in 1 nm increments. This EEM is divided into five regions based on historic data of where universal peaks of specific organic fractions appear. The region descriptions and absorbance ranges are presented in Table 2.2 and shown visually in Figure 2.3.

Table 2.2: FRI Region Breakdown

EEM Region	Description	Emission Range	Excitation Range
Region I	Aromatic Protein-like 1	280 – 330 nm	200 - 250 nm
Region II	Aromatic Protein-like 2	330 – 380 nm	200 - 250 nm
Region III	Fulvic acid-like	380 – 600 nm	200 - 250 nm
Region IV	Microbial byproduct-like	280 – 380 nm	250 - 340 nm
Region V	Humic acid-like	380 – 600 nm	250 - 400 nm

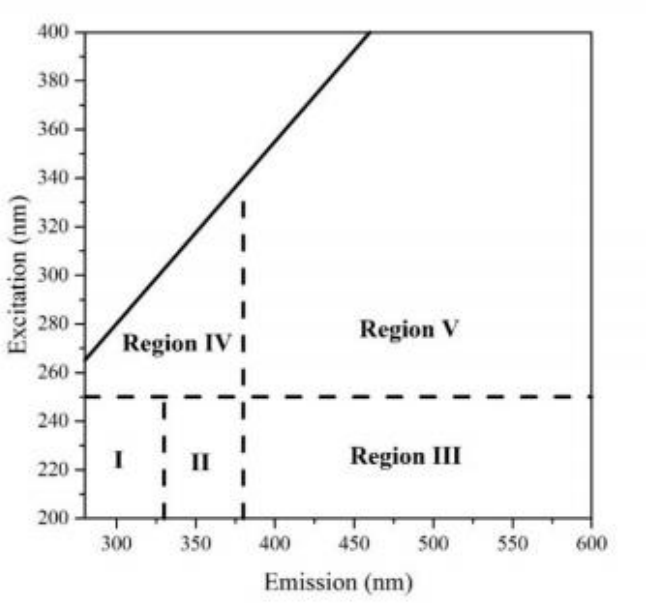

Figure 2.3: Fluorescence Regional Integration Legend

As defined by Chen and colleagues (2003), the volume under each region was determined by integration under the three dimensional EEM curve. The integration method consisted of the summation of the areas of the 1 by 5 nm squares (from the 1 and 5 nm measurement increments for emission and excitation wavelengths respectively) multiplied by the intensity (in arbitrary units (AU)) for the data points in each region. Equation 2-2 represents the formula used to quantify the volume of the discrete data set.

$$°_i = \Sigma_{ex}\Sigma_{em} I(Ï_{ex}Ï_{em})¢Ï_{ex}¢Ï_{em} \quad (2\text{-}2)$$

In Equation 2-2, $°_i$ represents the volume for a discrete set of data, while $¢Ï_{ex}$ is the excitation wavelength interval (5 nm), $¢Ï_{em}$ is the emission wavelength interval (1 nm), and $I(Ï_{ex}Ï_{em})$ is the fluorescence intensity at each excitation-emission pair. The volume under each region can be denoted by $\Sigma°_i$ bounded by the limits of each region which were outlined in Table 2.2.

As with any method of quantitative fluorescence analysis, background noise should be accounted for to accurately represent the organic composition of a water sample. In the case of the FRI method, Raman scattering as well as first and second order Raleigh scattering are the primary obstacle in obtaining quality results. First order Raleigh scattering is shown as the band on the EEM where emission equals excitation while second order Raleigh scattering occurs when emission equals twice that of the excitation. Raman scattering is described as a variation in energy difference from first order Rayleigh scattering which is dependent on the solvent (Rinnan et al., 2005). These scattering effects are accounted for primarily through blank subtraction but alternative methods of replacing missing data with three dimensional interpolation have been proposed with promising results (Bahram et al., 2006).

Alternatively, intensity values obtained through fluorescence spectroscopy can be spectrally corrected to the Raman scattering band as a method of accounting for this particular form of scattering as well as allowing for data to be comparable between multiple data sets instead of just internally. This correction changes the intensity unit from the original arbitrary units (AU) to Raman units (RU). The Raman scattering peak can be shown in the fluorescence analysis of a blank sample of deionized water at an excitation of 350 nm and an emission range of 375 to 420 nm. The area under this peak can be used using Equation 2-3 to convert the intensity of a data point from AU to RU (Lawaetz et al., 2009).

$$F_{\lambda_{ex}\lambda_{em}}(R.U.) = \frac{I_{\lambda_{ex}\lambda_{em}}(A.U.)}{A_{rp}} \qquad (2\text{-}3)$$

In Equation 2-3, $F_{\lambda_{ex}\lambda_{em}}(R.U.)$ is the fluorescence intensity normalized to the Raman peak, $I_{\lambda_{ex}\lambda_{em}}(A.U.)$ represents the intensity in arbitrary units, and A_{rp} is the area under the Raman peak using the aforementioned excitation and emission limits.

This technique is useful for comparison of data sets run on different spectrofluorometers due to instrument variability affecting results that are reported in AU. However, it has been shown by Bahram and colleagues (2006) that the subtraction of an EEM of a solvent blank will minimize the effects of Raman scattering for samples run on the same spectrofluorometer.

Relationship between Fluorescence and DBPs

Previous efforts to utilize fluorescence analysis to characterize organic matter in drinking water treatment with regards to DBPs have been explored. Bridgeman and colleagues (2011) provided a review of literature regarding previous studies that have applied fluorescence spectroscopy to characterize changes in NOM after disinfection in drinking water treatment. From the literature cited, only two studies had been conducted using FRI to correlate FEEM to DBPs (Bridgeman et al., 2011).

Yang and colleagues (2008) studied the correlation between NOM properties and DBP formation during chloramination using FRI and SUVA analysis. In this study, four DBPs were analyzed: 1) dichloroacetic acid, 2) chloroform, 3) dichloroacetonitrile, and 4) total organic halogen (TOX). FRI was used to correlate normalized FEEM volumes to the four aforementioned DBPs at four surface water locations. Results indicated that the cumulative normalized FEEM volumes for the aromatic protein and microbial byproduct-like fractions (regions II and IV) showed the strongest linear relationships with the DBPs studied (R^2 ranging from 0.42 to 0.63) (Yang et al., 2008). This

study revealed that for regions I, III, and V of the FEEM for the surface waters tested, no statistically significant correlation could be observed to the formation of the DBPs analyzed. The results presented by Yang et al. (2008) revealed a weak correlation between fluorescence and DBP formation using FRI, however, further research could be conducted to evaluate the use of correlating fluorescence spectroscopy in groundwaters to different regulated DBPs.

Johnstone and colleague (2009) furthered this research by using FRI and chlorine consumption to predict TTHM and HAA formation. In this research, a model was created using FEEM data to predict formation of chloroform, dichloroacetic acid, and trichloroacetic acid with linear relationships ranging from 0.33 to 0.75. A second model was created to determine if a combination of FRI (regions II, III, and IV) and chlorine consumption would increase the linear relationship to the formation of the aforementioned DBPs. Results indicated that the addition of chlorine consumption to the model increased linear relationships to values ranging from 0.82 to 0.92 (Johnstone et al., 2009).

While the studies conducted by Yang (2008) and Johnstone (2009) specifically targeted the use of FEEM to characterize DBP formation, the results were not compared to other commonly used organic analyses such as DOC and UV_{254}. A study conducted by Pifer and colleagues (2014) compared the suitability of DOC, UV_{254}, and FEEM as surrogate parameters to predict TTHM formation in raw and treated drinking water sources. For this research, a PARAFAC analysis was used to analyze FEEM data as opposed to FRI. Results revealed that UV_{254} ($r^2 = 0.89$) had the strongest correlation to TTHM formation when compared to the humic and fulvic component of the PARAFAC analysis ($r^2 = 0.78$) and DOC ($r^2 = 0.75$) (Pifer et al., 2014). The water sources analyzed included source waters from eleven WTFs located within watersheds underlain by six

different soil orders and coagulated with alum at pH 6, 7, and 8. A similar study conducted by Peleato and colleagues (2015) also compared the use of fluorescence analysis to DOC, UV_{254}, and SUVA. The study included modeling THMs with each of the organic analysis and comparing the plot of the predicted values to the actual recorded values. Results indicated that FEEM principle component analysis (PCA) was a strong indicator of NOM reactivity and DBP formation but that further studies needed to be conducted for a wide variety of source waters (Peleato et al., 2015).

The correlation results collected from the four aforementioned studies indicate variability in the observed relationships. With regards to fluorescence data, results for Pifer et al. (2014) and Peleato et al. (2015) indicated that the fulvic and humic fractions had the strongest correlation to TTHM formation compared to the other fractions of NOM. This is compared to Yang et al. (2008) and Johnstone et al. (2009), whom observed that aromatic proteins and microbial byproduct-like compounds showed a higher correlations to DBP formation. Correlation results also had high fluctuation as linear relationships ranging from 0.33 to 0.92 were observed for various organic parameters in relation to DBP formation. Discrepancies in results indicate that further investigation of the correlation of fluorescence data to DBP formation is required in order to obtain a more robust understanding of the use of FEEMs in drinking water treatment.

CHAPTER 3: SOURCE WATER CONDITIONS

This chapter describes the locations where groundwater samples were collected for testing in support of the research. The groundwater wells sampled supplied a variety of Florida water treatment facilities that were located in Polk County, Lake County, and Jupiter.

Lake Utility Services in Lake County, Florida

The groundwater wells sampled in Lake County Florida provided the majority of the source water used for experimentation. Eleven (11) wells were selected along US 27 and State Road Hwy 50 which were reported to have elevated THM precursor material. Ten of the wells draw water from the upper Floridan aquifer while the remaining well (Lake Groves 3) draws from the lower Floridan aquifer. The primary treatment for wells using the upper Floridan aquifer was disinfection with sodium hypochlorite prior to discharge into the distribution system. The lower Floridan aquifer is known to contain elevated levels of hydrogen sulfide, therefore, the Lake Groves 3 well is treated by packed tower aeration in addition to disinfection. A schematic illustrating the geographical locations of the wells are presented in Figure 3.1 while a list of the well names and abbreviations used for each well herein are presented in Table 3.1.

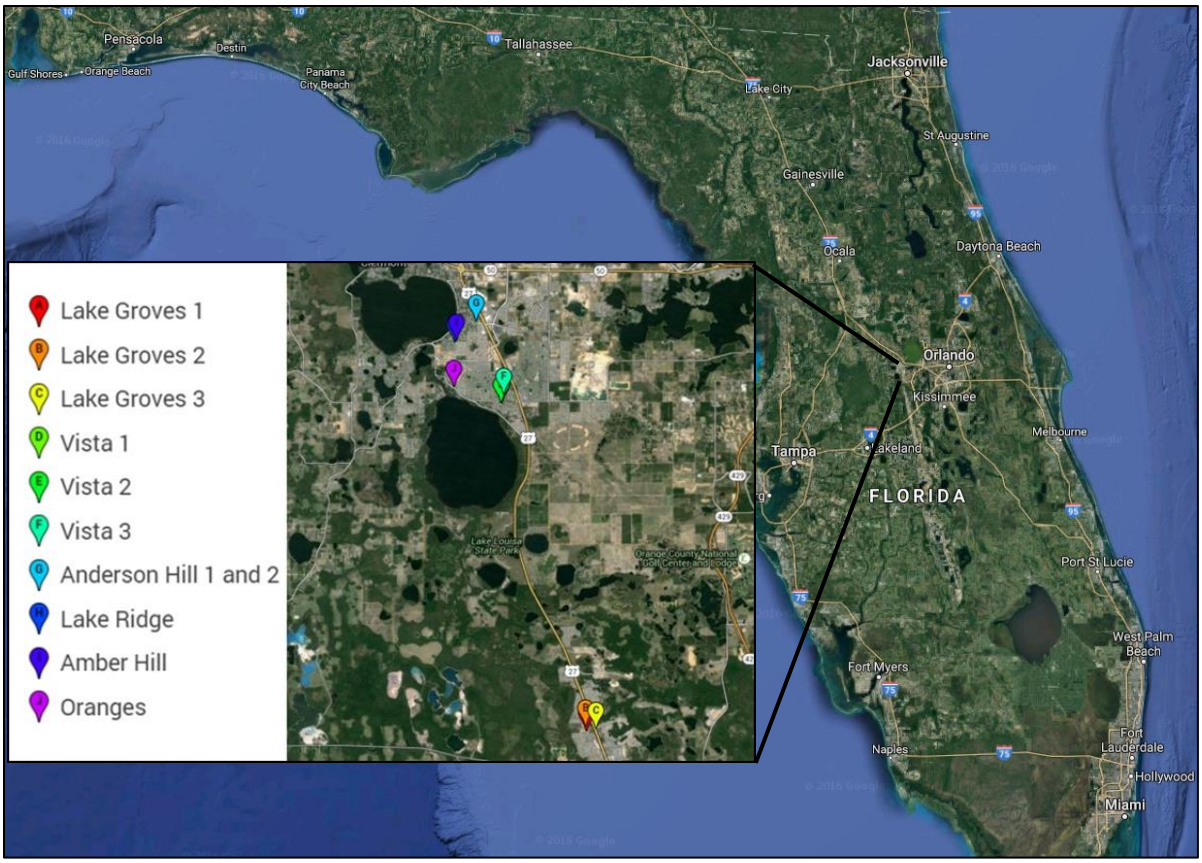

Figure 3.1: Geographical Locations of Sample Sites in Lake County FL

Table 3.1: Lake County Well Names and Abbreviations

Source Water Location	Sample ID
Vista 1	V1
Vista 2	V2
Vista 3	V3
Lake Groves 1	LG1
Lake Groves 2	LG2
Lake Groves 3	LG3
Oranges/Lake Louisa	OLL
Amber Hill	AMH
Lake Ridge	LR
Anderson Hill 1	AH1
Anderson Hill 2	AH2

Sampling occurred on January 21, 2016 and the water quality data collected is provided in Table 3.2 and Table 3.3.

Table 3.2: Lake County Field Water Quality

Well ID	Conductivity (µS/cm)	Temperature (°C)	pH	Turbidity (NTU)	True Color (PCU)	UV_{254} (cm^{-1})	Sulfides (mg/L)
LG1	517 ± 0	23.6 ± 0.2	7.50 ± 0.01	4.65 ± 0.35	< 5	0.038	BDL
LG2	482 ± 2	22.8 ± 0.2	7.48 ± 0.03	0.44 ± 0.04	< 5	0.038	0.16 ± 0.1
LG3	504 ± 1	24.7 ± 0.2	7.56 ± 0.02	0.21 ± 0.03	< 5	0.096	5.68 ± 0
V1	378 ± 1	23.1 ± 0.2	7.31 ± 0.04	0.21 ± 0.03	< 5	0.032	BDL*
V2	419 ± 1	22.7 ± 0.2	7.51 ± 0.01	0.33 ± 0.04	< 5	0.029	0.21 ± 0.1
V3	326 ± 0	23.1 ± 0.1	7.77 ± 0.05	0.71 ± 0.04	< 5	0.079	0.17 ± 0.1
OLL	313 ± 1	23.1 ± 0.1	8.08 ± 0.07	0.10 ± 0.02	< 5	0.081	0.2 ± 0.3
AMH	400 ± 1	23.1 ± 0.2	7.98 ± 0.04	0.12 ± 0.09	< 5	0.042	0.2 ± 0.2
LR	433 ± 1	23.2 ± 0.1	7.73 ± 0.01	0.09 ± 0.06	< 5	0.023	BDL*
AH1	208 ± 1	24.1 ± 0.4	8.33 ± 0.31	0.49 ± 0.03	< 5	0.061	0.14 ± 0
AH2	329 ± 0	23.8 ± 0.1	7.92 ± 0.02	0.26 ± 0.02	< 5	0.013	0.1 ± 0

*Below Detection Limit (BDL)

Table 3.3: Lake County Laboratory Analyzed Water Quality

Well ID	Calcium (mg/L)	Magnesium (mg/L)	Sodium (mg/L)	Iron (mg/L)	Chloride (mg/L)	Sulfate (mg/L)	Bromide (mg/L)	TDS (mg/L)	DOC (mg/L)
LG1	62.5	11.8	25.5	0.02	34	59	< 0.2	0.285	1.49
LG2	0.05	57.8	10.9	25.1	29	39	< 0.2	0.271	1.42
LG3	0.01	70.9	17.6	6.2	10	131	< 0.2	0.361	1.86
V1	46.2	10.9	10.9	0.01	22	28	< 0.2	0.190	1.17
V2	54.0	11.8	10.7	< 0.005	22	28	< 0.2	0.222	1.12
V3	40.0	12.2	6.9	0.03	14	13	< 0.2	0.168	2.29
OLL	45.0	8.7	5.2	0.03	12	8	< 0.2	0.220	2.78
AMH	54.6	12.2	8.0	0.04	18	32	< 0.2	0.157	1.44
LR	56.1	14.1	9.1	0.02	21	37	< 0.2	0.229	0.89
AH1	24.5	7.2	4.5	0.03	9	6	< 0.2	0.102	2.06
AH2	37.5	9.6	9.6	< 0.005	22	25	< 0.2	0.159	0.56

Polk County Utilities in Polk County, Florida

The sampling location located in Polk County Florida was the Babson Park Water Treatment Facility 2 (BP2). BP2 utilizes a single groundwater well that draws from the Floridan aquifer as a source water. The treatment process consists of a granular activated carbon bed followed by disinfection with sodium hypochlorite in conjunction with hydrogen sulfide removal via tray aerators. The treated water is stored in the on-site ground storage tank prior to being pumped into the distribution system. A process schematic is provided in Figure 3.2 and water quality is presented in Table 3.4.

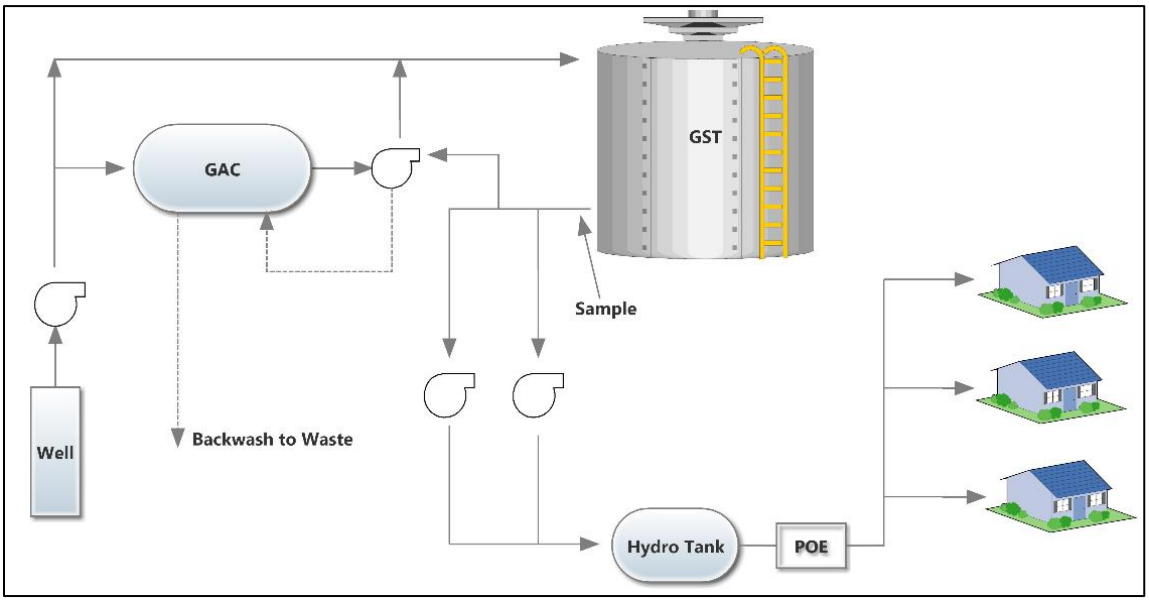

Figure 3.2: Babson Park Process Flow Schematic

Table 3.4: Babson Park Water Quality

Water Quality Parameter	Value
pH	7.41
Temperature (°C)	25.7-26.7
Hardness (mg/L)	54-65
Alkalinity (mg/L)	61-76
Ortho Phosphate as PO_4 (mg/L)	1.10-1.90
Bromide (mg/L)	BDL* (<0.05)
Arsenic (ppb*)	0.24-0.37
Barium (ppm*)	0.01-0.02
Cyanide (ppb)	ND*-3.50
Fluoride (ppm)	0.061-0.084
Lead (ppb)	ND*-0.063
Selenium (ppb)	0.66-1 .00
Sodium (ppm)	19.0-20.0
Thallium (ppb)	ND*-0.031

*Not Detectable (ND)
*Below Detection Limit (BDL)
*parts per million (ppm)
*parts per billion (ppb)

Jupiter Water Utilities in West Palm Beach, Florida

The town of Jupiter is located in West Palm Beach, Florida. In comparison to the aforementioned sites, the water production facility in Jupiter is more sophisticated, utilizing sand filtration, cartridge filtration, ion exchange, acid reduction, as well as nanofiltration and reverse osmosis membrane treatment. The water source sampled for experimentation was the influent water to the treatment facility which is taken from a surficial well. A process schematic for the water treatment facility is provided in Figure 3.3 and water quality is presented in Table 3.5.

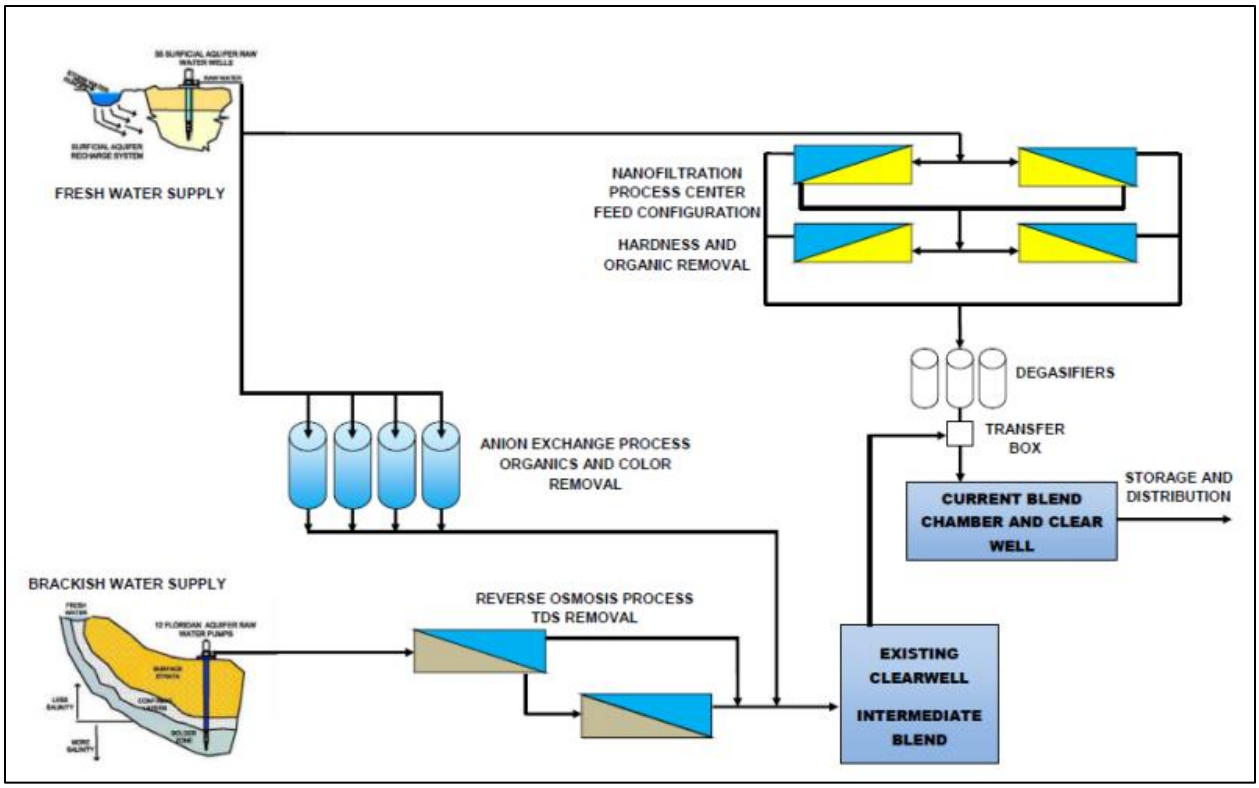

Figure 3.3: Jupiter WTF Process Flow Schematic

Table 3.5: Jupiter WTF Water Quality

Water Quality Parameter	Value
pH	7.05
Temperature (°C)	27.2
Conductivity (µS/cm)	756.9
Turbidity (NTU)	0.19
Color (CU)	36 – 38
Hardness (mg/L $CaCO_3$)	328
Alkalinity (mg/L)	300 – 307
Sulfate (mg/L)	25
Chloride (mg/L)	53
Calcium (mg/L)	113
Magnesium (mg/L)	4.6
Sodium (mg/L)	21
Silica (mg/L)	11

CHAPTER 4: MATERIALS AND METHODS

The ability to correlate DBP formation in a drinking water distribution system to source water NPOC will assist water purveyors in projecting TTHM and HAA content in their system. This would be beneficial when the water purveyors alter or extend the water distribution system, as these actions will impact formation potential. Additionally, should a water purveyor place on-line new wellfields, fluorescence data could be used to project DBP content changes in the system.

Research involving dosing studies on raw, untreated water is one method of understanding formation potential under conservative conditions such as high temperature, long residence times, and MRDL chlorine doses. UCF coordinated with Florida drinking water utilities in Polk County, Lake County, and Jupiter to perform a number of dosing studies on various wells to assess the DBPs in the distribution systems. The data collected from these studies was used to compare the effectiveness of ultraviolet absorption and fluorescence spectroscopy to characterize organic content that then could be correlated to TTHM formation.

This chapter is divided into two sections: 1) methods describing a chlorine dosing study for TTHM formation analysis and 2) methods describing the characterization of NPOC using fluorescence spectroscopy and ultraviolet absorption. Each section herein describes the experimental plan, testing methodology, materials, chemicals, and procedures implemented in this study.

Chlorine Dosing Evaluation and TTHM Formation Analysis

Experimental Plan

Bulk raw water samples were taken from each of the fifteen sampling locations and transported back to UCF laboratories for analysis. Each set of samples were evaluated for raw water quality,

organic content, chlorine demand, and TTHM formation potential. The locations and timeframe during which each of the samples were collected and analyzed are presented in Table 4.1.

Table 4.1: Source Water Background Information

Source Water Location	Sample ID	Water Type	Collection Date
Lake County			
Vista 1	V1	Groundwater	January 21, 2016
Vista 2	V2	Groundwater	January 21, 2016
Vista 3	V3	Groundwater	January 21, 2016
Lake Groves 1	LG1	Groundwater	January 21, 2016
Lake Groves 2	LG2	Groundwater	January 21, 2016
Lake Groves 3	LG3	Groundwater	January 21, 2016
Oranges/Lake Louisa	OLL	Groundwater	January 21, 2016
Amber Hill	AMH	Groundwater	January 21, 2016
Lake Ridge	LR	Groundwater	January 21, 2016
Anderson Hill 1	AH1	Groundwater	January 21, 2016
Anderson Hill 2	AH2	Groundwater	January 21, 2016
Polk County			
Babson Park 2	BP2	Groundwater	July 27, 2016
West Palm Beach County			
Jupiter WTF	JUP	Surficial Aquifer	August 25, 2016

Once groundwater samples arrived at UCF laboratories, they were analyzed for source water quality parameters such as NPDOC, anions, cations, total dissolved solids (TDS), and UV_{254}. The remainder of the bulk water samples were aerated to remove the presence of sulfide and then stored at 4°C until further testing took place. Samples were dosed with a known concentration of sodium hypochlorite (bleach) and incubated at 30°C for the duration of the 4 day time series. Samples were analyzed for chlorine residual and TTHM concentration at pre-determined time intervals over the four day incubation period to determine chlorine demand and TTHM content of each sample.

Sample Collection

On each of the dates specified in Table 4.1, bulk water was collected and stored in 1L glass amber bottles from the source groundwater wells at each of the WTFs. These samples were transported

back to UCF laboratories and stored at 4°C until experimentation was conducted. Sample collection was performed in accordance with *Standard Methods for the Examination of Water and Wastewater* (American Public Health et al., 2005). Sections 1030B and 1030C were referenced for the collection of samples and for sample storage and preservation respectively.

Water Quality Testing Methodology and Equipment

Water quality analysis was conducted partly in the field and partly in the laboratory. Table 4.2 and Table 4.3 describes the method used in reference to *Standard Methods for the Examination of Water and Wastewater* (SM) as well as the equipment description and method detection level for each parameter analyzed.

Table 4.2: Field Analytical Methods, Equipment, and Detection Range

Analyte	Method and/or Equipment Description	Detection Level
pH	4500-H^+ B. Electrometric Method HQ40d Portable pH, Conductivity and Temperature Meter	0.01 pH Units
Temperature	2550 B. Laboratory and Field Methods HQ40d Portable pH, Conductivity and Temperature Meter	0.01 °C
Conductivity	2510 B. Laboratory Method HQ40d Portable pH, Conductivity and Temperature Meter	0.01 µS/cm
Turbidity	2130 B. Nephelometric Method Hach 2100q Portable Turbidimeter	0.01 NTU
True Color	2120 C. Spectrophotometric –Single Wavelength Method	1 PCU, >5
Total Sulfides	4500-S2-F. Iodometric Method	0.1 mg/L

Table 4.3: Laboratory Analytical Methods, Equipment, and Detection Range

Analyte	Method and/or Equipment Description	Detection Level
UV-254	5910 B. Ultraviolet Absorption Method	0.01 cm-1
DOC	5310 C. Persulfate-Ultraviolet Oxidation Method	0.25 mg/L
Total Dissolved Solids	2540 C. Total Dissolved Solids Dried at 180^{o}C	2.5 mg/L
Sulfate	4110 B. Ion Chromatography (IC) with Chemical Suppression of Eluent Conductivity	1 mg/L
Chloride	4110 B. Ion Chromatography (IC) with Chemical Suppression of Eluent Conductivity	1 mg/L
Bromide	4110 B. Ion Chromatography (IC) with Chemical Suppression of Eluent Conductivity	0.20 mg/L
Magnesium	3120 B. Inductively Coupled Plasma (ICP) Method	0.03 mg/L
Calcium	3120 B. Inductively Coupled Plasma (ICP) Method	0.01 mg/L
Sodium	3120 B. Inductively Coupled Plasma (ICP) Method	0.03 mg/L
Iron	3120 B. Inductively Coupled Plasma (ICP) Method	0.007 mg/L

Experimental Procedures

Remaining bulk water samples were aerated for sulfide removal upon arrival to UCF laboratories. Samples were aerated overnight (at least 12 hours) in 4L glass amber bottles using an AIR-1000 Topfin air pump with a porous diffusion stone at a flow rate of 0.22 gallon per minute (gpm). Total sulfide and chlorine contents were measured using Hach's Methylene Blue Method 8131 for sulfide analysis and Hach's DPD Method 8021 for free chlorine analysis to ensure that neither constituent was present.

After aeration, samples were dosed with concentrated sodium hypochlorite solution. The concentration of the sodium hypochlorite dose was determined such that a free chlorine residual of 4.00 $\pm$ 0.20 mg/L was obtained after a 15 minute contact time for each sample. This limit was chosen based on the D/DBP Rule regulations on disinfectant levels which states that the effluent disinfectant level for sodium hypochlorite cannot exceed 4.0 mg/L leaving the point of entry (POE)

of the WTF. It is noted that source water from Jupiter's surficial aquifer was highly concentrated with organic precursor material which resulted in a scenario in which a fifteen minute free chlorine residual of 4.0 mg/L and a four day residual greater than 0.20 mg/L could not be met. The source water was diluted by a factor of four so that the chlorine residual testing conditions could be achieved. Data acquired from the Jupiter sample henceforth is based on a four to one dilution factor of the original source water.

The determined doses are summarized in Table 4.4.

Table 4.4: Sodium Hypochlorite Dose

Source Water Location	Sample ID	Sodium Hypochlorite Dose (mg/L)
Lake County		
Vista 1	V1	4.5
Vista 2	V2	4.2
Vista 3	V3	6.2
Lake Groves 1	LG1	4.8
Lake Groves 2	LG2	5.0
Lake Groves 3	LG3	6.6
Oranges/Lake Louisa	OLL	6.4
Amber Hill	AMH	5.4
Lake Ridge	LR	4.6
Anderson Hill 1	AH1	6.1
Anderson Hill 2	AH2	4.2
Polk County		
Babson Park 2	BP2	6.5
West Palm Beach County		
Jupiter WTF	JUP	6.5

Using these doses, each aerated samples was transferred into a 2L glass volumetric flask and dosed with sodium hypochlorite. The dosed samples were mixed thoroughly and distributed among 60 mL glass amber bottles to represent free chlorine residual and TTHM aliquots for the following times: 15 minute, 8 hour, 24 hour, 48 hour, 72 hour, and 96 hour. Each bottle was filled to the top and capped with a Teflon lined septa cap to eliminate headspace and minimize aeration. A

duplicate analysis was included such that two separate 60 mL amber bottles were included for TTHM concentration analysis at each time point.

Samples were transferred and stored in a 30°C oven for incubation for the duration of the time series testing. The incubation temperature was chosen to simulate a distribution system located in a sub-tropical Florida climate (Duranceau et al., 2013). At each time period, the TTHM samples were removed from the incubator and quenched with sodium metabisulfite in order to consume the remaining chlorine residual and halt additional THM formation until the concentration could be analyzed. Aliquots were also analyzed for free chlorine residual in tandem with the quenching at each time period. Quenched samples were stored in a cooler at 4°C until the 96 hour sample had been quenched. After the samples had been quenched with sodium metabisulfite, TTHMs were analyzed using a gas chromatograph (GC) with a liquid – liquid extraction method with hexane as the extraction reagent.

The incubation temperature, detention time, and closed system nature of the sample bottles were intended to simulate a conservative scenario in a distribution system. However, the laboratory techniques do not take into account the many variables present in a full scale distribution system and therefore may not fully represent the conditions in an actual distribution system.

Organic Characterization with Fluorescence Spectroscopy and Ultraviolet Absorptions

Natural organic matter is the primary precursor to TTHM and HAA_5 formation, and as such, the characterization of naturally occurring organic content in source water can be analyzed and compared to the formation of DBPs. The organic composition of each of the raw source waters was determined using fluorescence spectroscopy, ultraviolet absorption (UV_{254}), and non-

purgeable dissolved organic carbon (NPDOC). Fluorescence was analyzed on a Shimadzu RF-6000 spectrofluorometer (Kyoto, Japan), UV_{254} on a Hach DR 5000 spectrophotometer (Loveland, CO), and NPDOC on a Teledyne Tekmar TOC Fusion (Mason, OH). The procedure for sample preparation, procedure, and data analysis for each organic measurement is described in greater detailed in the following sections.

Dissolved Organic Carbon Analysis

The dissolved organic content of each groundwater source was determined using method 5310C (American Public Health et al., 2005). Pretreatment consisted of filtering sample through a pre-washed, 0.45 μm diameter nitrocellulose membrane filter. Samples were analyzed within 48 hours and preserved at 4°C until analysis could take place.

Ultraviolet Absorption (UV_{254})

Ultraviolet absorption was measured for each sample at a wavelength of 254 nanometers (nm) using a Hach DR 5000 spectrometer. Sample was filtered in a pre-washed, 0.45 μm diameter Millipore nitrocellulose membrane filter and placed in a quartz cuvette and analyzed using method 5910 B (American Public Health et al., 2005).

Fluorescence Spectroscopy

Water from each of the sampling locations was transported to UCF laboratories and measured for fluorescence intensity within 24 hours; samples that were not read immediately were preserved at 4°C and read the following day. Sample pretreatment included filtering through a pre-washed 0.45 μm diameter Millipore nitrocellulose membrane filter in order to remove particulates. The fluorescence EEM was measured using a Shimadzu RF-6000 spectrofluorometer. The emission

and excitation bandwidths were set to 10 nm. The excitation wavelengths ranged from 200 to 400 nm in 5 nm increments while the emission wavelengths ranged from 280 to 600 nm in 1 nm increments. The intensity for each excitation emission pair was recorded and a three dimensional EEM plot was created for each sample.

Quantitative analysis of EEM data was performed using the fluorescence regional integration method (FRI) as defined by Chen et al. (2003). Each fluorescence scan was divided into five regions on the basis of general characterizations of organic matter from an accumulation of previous studies. The absorbance ranges of the regions as well as the organic description are provided in Table 2.2 and shown visually in Figure 2.3.

A blank correction factor was included to reduce the interference of Raleigh and Raman scattering by subtracting the fluorescence spectra obtained from a sample of deionized water. Data was analyzed in Microsoft Excel using the methodology presented by Chen et al. (2003) for the FRI method with the inclusion of the aforementioned correction factors to determine the normalized, integrated volume ($\varphi_{i,n}$) for each region.

Laboratory Quality Assurance and Control

The assessment of varying water quality parameters to quantify DBP formation and organic composition was ubiquitous throughout this study. Statistics and quality control analysis were calculated in accordance with *Standard Methods for the Examination of Water and Wastewater* 1010B. Statistics and 1020 B. Quality Control. The accuracy and reliability of the data collected throughout experimentation can be shown through the quality assurance and control conducted in tandem with experimental data.

Duplicate and replicate samples were analyzed to determine relative percent difference (RPD). RPD values were accepted in the ranges of 90 – 110% and is represented by Equation 4-1. Outliers were also identified and removed if a data point was greater than the mean plus three times the standard deviation of the data set.

$$RPD = \frac{S-D}{\left(\frac{S+D}{2}\right)} \cdot 100\% \quad (4\text{-}1)$$

$$S = Sample\ result\ \left(\frac{mg}{L}\right)$$

$$D = Duplicate\ sample\ result\ \left(\frac{mg}{L}\right)$$

Accuracy

Accuracy is the measurement of the consistency of an analytical method or instrument. To determine accuracy, a water sample is spiked with a known amount of the constituent being measured and compared against a sample that had not been spiked to determine instrument or method variability. Accuracy charts were constructed for the data sets measured for samples being measured for THM concentration by the GC using Equation 4-2. The percent recovery of each spiked sample was graphed and depicted as an accuracy chart.

$$\%\ Recovery = \frac{C_{sample+spike} - C_{sample}}{C_{spike}} \cdot 100\% \quad (4\text{-}2)$$

$$C_{sample+spike} = concentration\ of\ the\ spiked\ sample\ \left(\frac{mg}{L}\right)$$

$$C_{sample} = concentration\ of\ the\ sample\ \left(\frac{mg}{L}\right)$$

$$C_{spike} = concentration\ of\ the\ spike\ \left(\frac{mg}{L}\right)$$

Upper warning levels (UWL), lower warning levels (LWL), upper control levels (UCL), and lower control levels (LCL) were included in the accuracy chart. The warning limits are defined as limits plus or minus two standard deviations from the mean while the control limits are defined to be limits plus or minus three standard deviations from the mean of the data set. The equations for the WL and the CL are shown in Equations 4-3 and 4-4, respectively.

$$WL = \bar{x} \pm 2s \tag{4-3}$$

$$CL = \bar{x} \pm 3s \tag{4-4}$$

$\bar{x} = mean\ of\ the\ percent\ recovery$

$s = standard\ deviation\ of\ the\ percent\ recovery$

Data points that fell above the UCL or below the LCL were considered inaccurate and were removed from the data set. In the case that two or more consecutive data points exceeded the WLs, the samples were re-analyzed and/or were removed from the data set.

Precision

Precision is the measurement of reproducibility between samples and duplicate samples. A precision chart was constructed from average and standard deviation values to determine variation. The industrial statistic (I-statistic) was used to create precision control charts for THM analysis using Equation 4-5.

$$I = \frac{|S-D|}{S+D} \tag{4-5}$$

$S = sample\ result\ \left(\frac{mg}{L}\right)$

$D = duplicate\ sample\ result\ \left(\frac{mg}{L}\right)$

Upper control limits (UCL) and upper warning limits (UWL) were included in the precision charts and defined as the average I-statistic value plus three and two standard deviations for the CL and WL respectively. The equations used to calculate the UCL and UWL are shown in Equations 4-6 and 4-7, respectively.

$$UCL = I_{avg} + 3s \tag{4-6}$$

$$UWL = I_{avg} + 2s \tag{4-7}$$

$I_{avg} = average\ of\ the\ I_{stat}\ values$

$s = standard\ deviation\ of\ the\ I_{stat} values$

Data points that fell above the UCL or below the LCL were removed from the data set. In the case that two or more consecutive data points exceeded the WLs, the samples were re-analyzed and/or removed from the data set.

CHAPTER 5: RESULTS AND DISCUSSION

The data collected in this research included water quality, TTHM concentration, and organic analysis through the use of DOC, ultraviolet absorbance, and fluorescence spectroscopy. Water quality data has been provided in Appendix A while the remaining data are presented in the following sections of this chapter. Correlation data is also provided to show the relationship of the two main data sets: 1) four day TTHM concentration and 2) organic composition and analysis.

Simulated Distribution System Analysis

A simulated distribution system analysis was conducted for each of the raw water samples in which aeration pretreatment followed by sodium hypochlorite dosing were performed. Samples were allowed to incubate at 30°C to represent summer conditions in a Florida drinking water distribution system and stored in 60 mL glass amber bottles with no headspace to simulate water in a closed pipe system. During the incubation time of four days, the free chlorine residual and TTHM concentration were monitored at specified intervals. Free chlorine data was recorded to ensure that residual did not decrease below 0.2 mg/L for which case the dosing procedure would need to be repeated with a higher dose of sodium hypochlorite. The results of this analysis are presented in the following sections and include a discussion of the chlorine decay data and TTHM data.

Free Chlorine Monitoring

Raw groundwater from each of the sample locations was aerated and dosed with sodium hypochlorite in accordance with the experimental procedures outlined in Chapter 4. The initial instantaneous chlorine demand takes place rapidly once the sodium hypochlorite is introduced to the water sample, during which, the free chlorine residual quickly decreases in the first fifteen minutes of contact time. This demand is typically due to the presence of reducing compounds such

as iron and manganese which react with the chlorine to form insoluble oxides. The samples maintained a free chlorine residual of 4.0 ± 0.20 mg/L after this fifteen minute time span even though the initial sodium hypochlorite dose ranged from 4.2 to 7.5 mg/L. The majority of the reaction chemistry takes place at slower rate over a longer period of time and is due to reaction with natural organic matter (NOM) in the water sample. Chlorine residuals at the end of the four day incubation period ranged from a high of 3.24 to a low of 0.88 mg/L for AH2 and V3, respectively. This resulted in a total chlorine demand of 5.62 mg/L for the V3 well and a demand of 1.06 mg/L for AH2 with the remaining samples ranging in between. Figure 5.1 depicts the monitoring of the free chlorine residual over the incubation period.

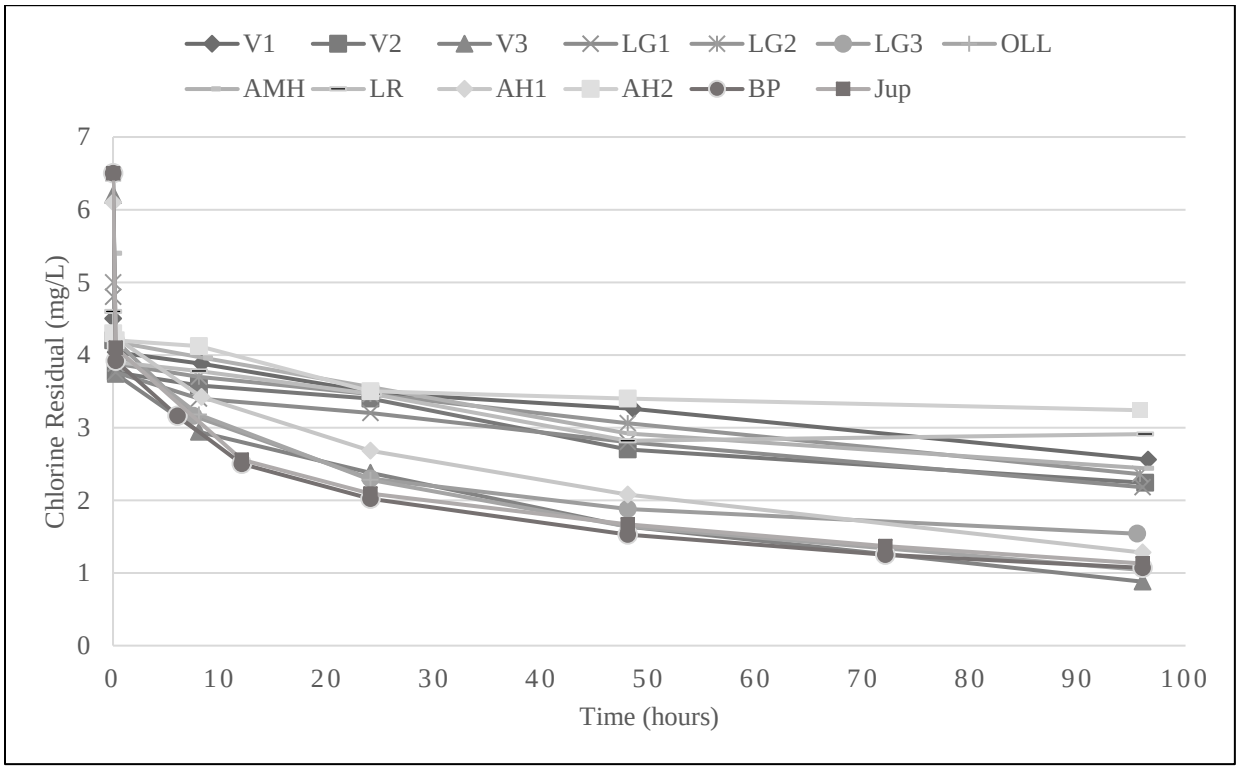

Figure 5.1: Four Day Chlorine Decay Curves

TTHM Concentration Analysis

The TTHM formation potential for each of the source waters was determined by plotting the TTHM concentrations obtained through experimentation against time. Each data point was determined based on the average TTHM concentration of a duplicate analysis and analyzed via gas chromatography. Samples were quenched with sodium metabisulfate at each of the specified times to consume the remaining chlorine until the samples could be analyzed for TTHM concentration using gas chromatography. The TTHM formations over the four day incubation period are presented in Figure 5.2 based on data presented in Appendix B. The MCL at 80 ppb is shown in conjunction with the TTHM formation curves as a visual representation of the approximate time samples exceeded the limit over the duration of the incubation period.

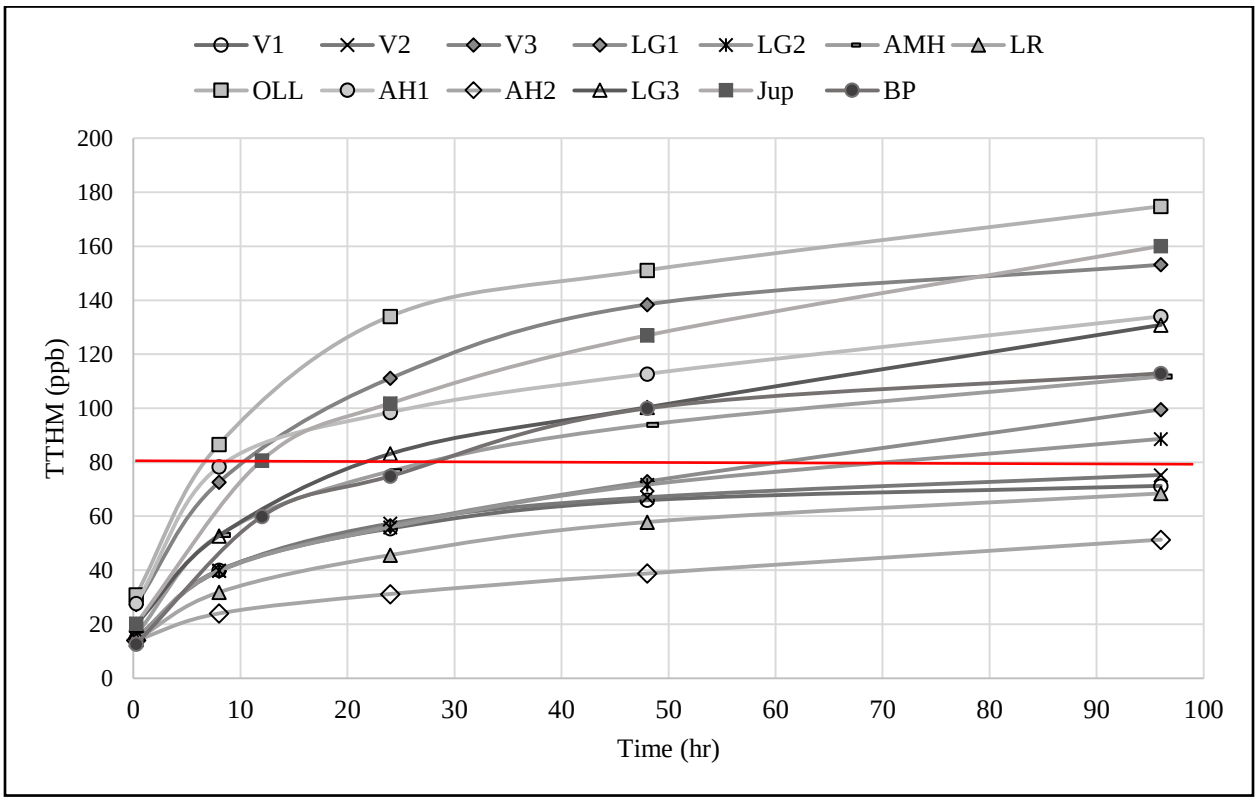

Figure 5.2: Four Day TTHM Formation Curves

Results show that the ultimate TTHM concentrations ranged from 51 ppb to 175 ppb with four samples under the MCL after four days and the remaining exceeding the limit anywhere between 7 to 70 hours after the introduction of the sodium hypochlorite disinfectant. The samples that showed particularly high ultimate TTHM concentrations were OLL, Jupiter, AH1, V3, and LG3 which had four day TTHM concentrations of at least 130 ppb. The four samples that had four day TTHM concentrations below the MCL were AH2, LR, V1, and V2 from lowest to highest concentration respectively. The wells that resulted in high and low TTHM concentrations will be the focus of comparison in the following sections.

Organic Composition Results and Correlations

The following sections will present the results from the organics analysis of the sample set using data collected from the dissolved organic carbon, ultraviolet absorbance, and fluorescence spectroscopy analysis. Each section will address the nature of the analysis in regards to how the organics are being characterized, present the results from each analysis, as well as a correlation between the data set and the aforementioned TTHM concentration results. Each correlation will produce a linear and second order polynomial coefficient of determination (R^2) which will serve as means of comparison to show which organic analysis has the strongest relationship to four day TTHM concentration.

Dissolved Organic Carbon Analysis

DOC represents the dissolved fraction of the TOC and is the primary parameter for measuring TTHM precursors in this work. DOC was determined by filtering samples through a pre-washed 0.45 μm microcellulose membrane filter and analysis using a Teledyne Tekmar Fusion Total

Organic Carbon Analyzer. Results for the DOC concentrations for each sample are presented in Table 5.1 alongside four day TTHM concentration.

Table 5.1: Dissolved Organic Carbon Results

Sample ID	Average DOC Concentration (mg/L)	Four day TTHM Concentration (ppb)
Jup	2.77 ± 0.05	160.1
OLL	2.77 ± 0.02	174.8
V3	2.27 ± 0.03	153.2
AH1	2.08 ± 0.04	134.0
BP2	2.10 ± 0.09	112.9
LG3	1.88 ± 0.04	130.9
LG1	1.49 ± 0.01	99.6
AMH	1.42 ± 0.03	111.7
LG2	1.41 ± 0.02	88.6
V1	1.18 ± 0.02	71.2
V2	1.11 ± 0.01	75.3
LR	0.89 ± 0.01	68.4
AH2	0.55 ± 0.01	51.3

The DOC concentrations ranged from 2.77 to 0.55 mg/L. The Jupiter and OLL samples showed marginally higher DOC concentrations while the LR and AH2 showed particularly low DOC concentrations. These results are similar to the trends seen in the four-day THM concentrations. Correlation results are presented in Figure 5.3 and Figure 5.4 for which the DOC results are plotted against the TTHM four-day concentration results to determine the linear and second order polynomial coefficients of determination (R^2), respectively.

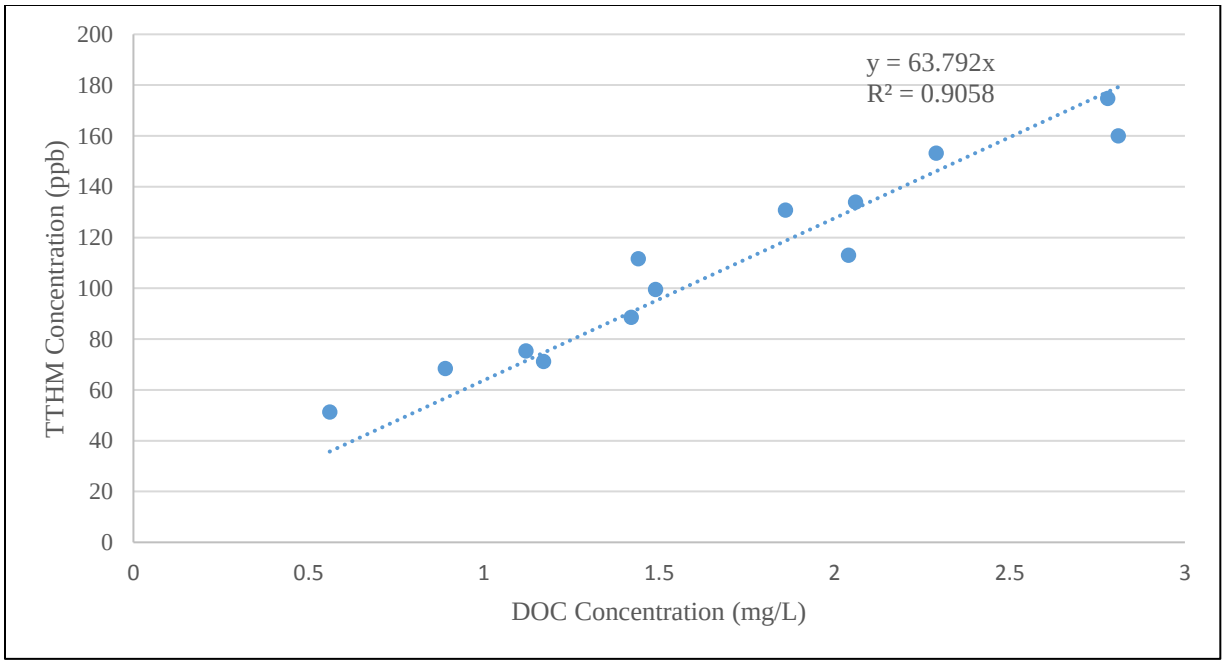

Figure 5.3: Linear Regression Correlation for DOC and 4 Day TTHM Concentration

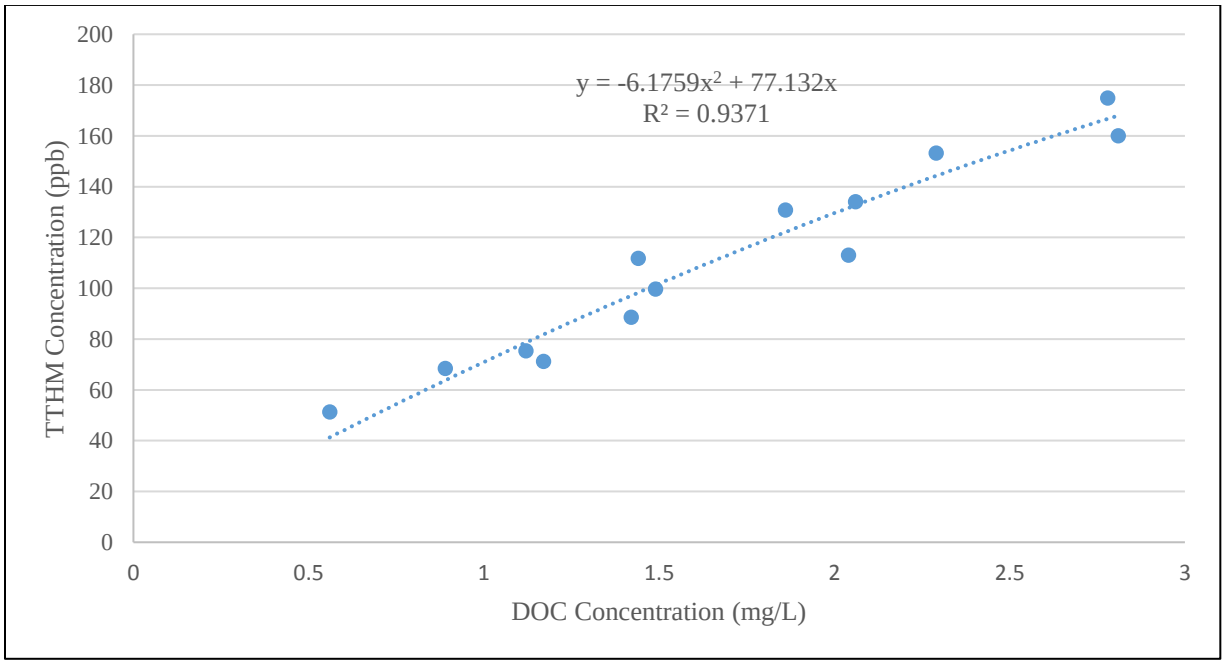

Figure 5.4: Polynomial Regression Correlation for DOC and 4 Day TTHM Concentration

The R^2 for the correlation between DOC and four day TTHM content was shown to be 0.906 for the linear regression and 0.937 for the second order polynomial regression. Both regressions revealed a strong correlation between DOC and four day TTHM content with the second order polynomial regression having a higher R^2 and fitting better to the higher DOC values.

Ultraviolet Absorbance (UV_{254}) Analysis

Ultraviolet absorbance at a wavelength of 254 nanometers (UV_{254}) has been widely used in the drinking water industry to provide an indication of the concentration of organic matter in a sample of water. The advantage of UV_{254} is such that it specifically measures organic matter that contains aromatic rings such as humic and fulvic substances, both of which are known to be major precursors for DBP formation. Samples were filtered through a pre-washed 0.45 µm membrane filter to control particle-related variations in the UV absorption. Results for the UV_{254} absorbance are presented in Table 5.2 alongside four day TTHM concentration.

Table 5.2: Ultraviolet Absorbance (UV_{254}) Results

Sample ID	Average UV_{254} Absorbance (cm^{-1})	Four Day TTHM Concentration (ppb)
JUP	0.100 ± 0.001	160.1
LG3	0.096 ± 0.000	130.9
OLL	0.081 ± 0.000	174.8
V3	0.079 ± 0.001	153.2
AH1	0.061 ± 0.000	134.0
BP2	0.053 ± 0.001	112.9
AMH	0.042 ± 0.001	111.7
LG1	0.038 ± 0.000	99.6
LG2	0.038 ± 0.001	88.6
V1	0.032 ± 0.000	71.2
V2	0.029 ± 0.001	75.3
LR	0.023 ± 0.001	68.4
AH2	0.013 ± 0.000	51.3

Results show that the samples with the five highest UV_{254} absorbance also had the highest four-day TTHM concentration. However, the top five samples on both lists did not occur in the same order as OLL had the highest TTHM concentration but only the third highest UV_{254} absorbance of the data set. This is also reflected in LG3 which had the second highest UV_{254} absorbance but only the fifth highest TTHM concentration. Figure 5.5 and Figure 5.6 plot the UV_{254} absorbance data against TTHM concentration to determine the linear and second order polynomial R^2 coefficients, respectively.

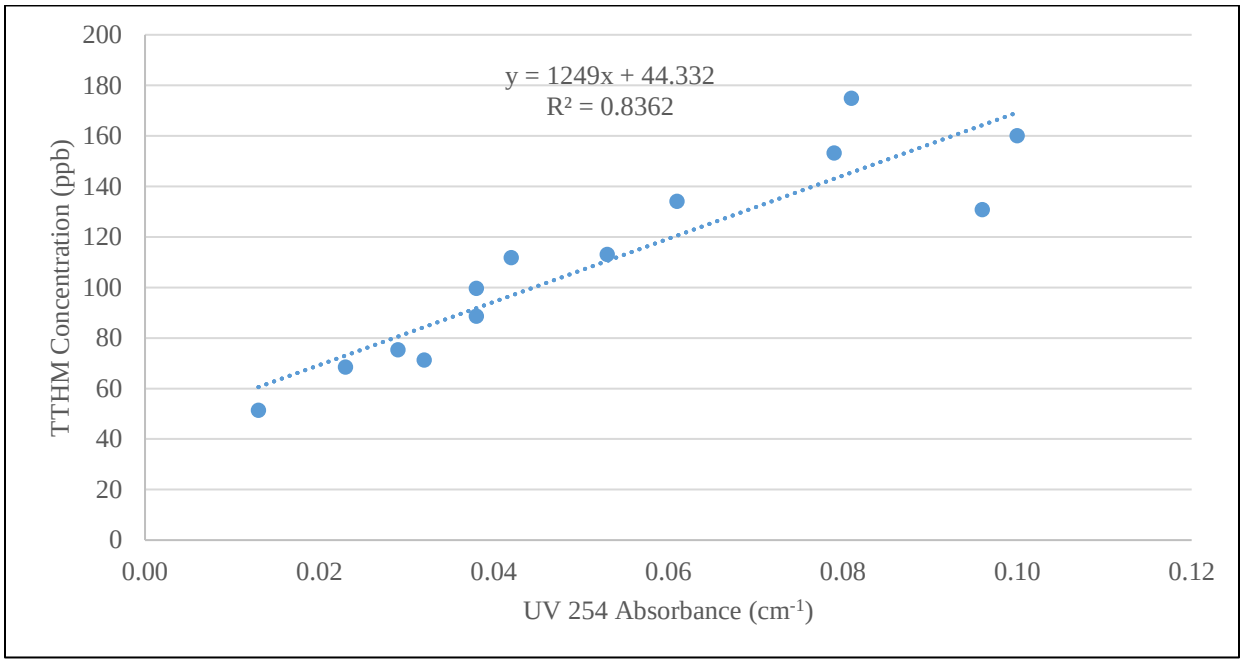

Figure 5.5: Linear Regression Correlation for UV_{254} to 4 day TTHM Concentration

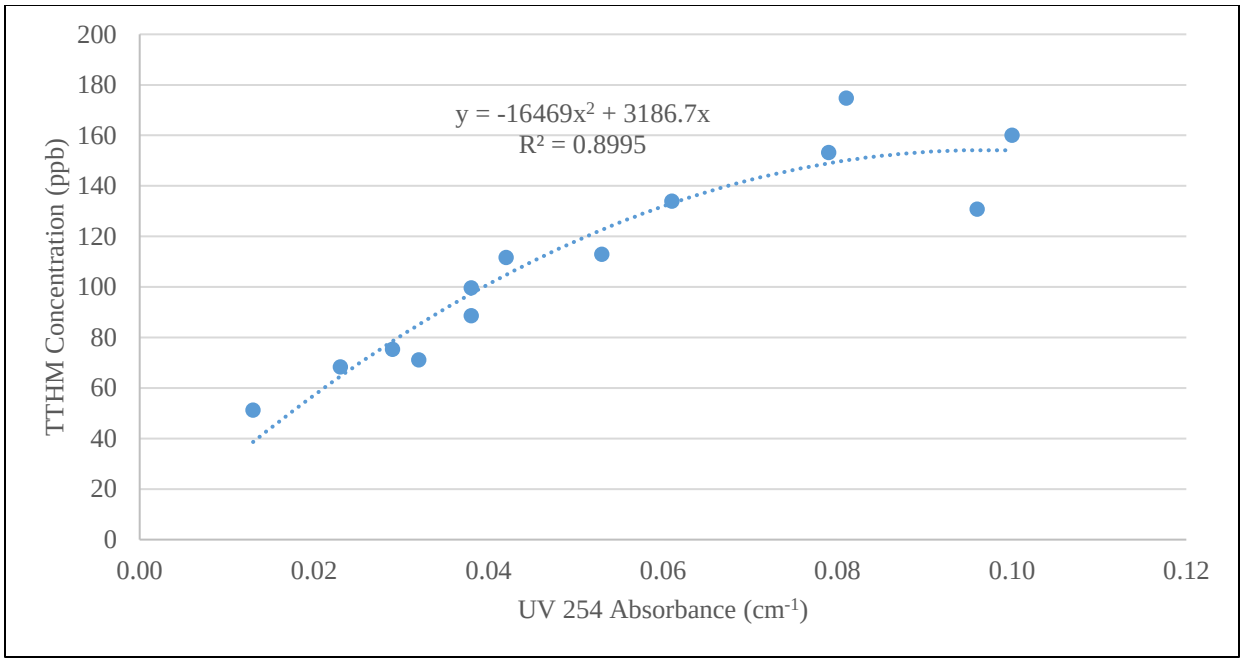

Figure 5.6: Polynomial Regression Correlation to UV_{254} and 4 Day TTHM Content

The linear R^2 for UV_{254} absorbance was shown to be 0.836 while the second order polynomial regression revealed an improved R^2 of 0.90. These values were lower than the coefficients shown in correlation between DOC and four day TTHM concentration. A noteworthy observation is that if the top two data points (JUP and LG3) are removed from the UV_{254} correlation data set the coefficient of determination increases to 0.963 which is higher than that for DOC. This may show a limitation in using UV_{254} absorbance as an indicator for DBP precursors for source waters that contain organics with high aromaticity.

Specific Ultraviolet Absorbance (SUVA)

The SUVA values were determined by dividing the UV_{254} results by the DOC results and converting the units to mg/L/m. Results for the SUVA values for each sample are presented in Table 5.3 alongside four day TTHM concentration.

Table 5.3 Specific Ultraviolet Absorbance (SUVA) Results

Sample ID	SUVA (mg/L/m)	Four day TTHM Concentration (ppb)
LG3	5.16	130.8
JUP	3.56	160.1
V3	3.45	153.2
AH1	2.96	134
AMH	2.92	111.7
OLL	2.91	174.8
V1	2.74	71.2
LG2	2.68	88.6
BP2	2.60	113
V2	2.59	75.3
LR	2.58	68.4
LG1	2.55	99.6
AH2	2.32	51.3

SUVA results ranged from 2.32 to 5.16 mg/L/m with an average of 3.00 mg/L/m. LG3 deviated from the rest of the data extending 2.93 standard deviations above the mean. This value was removed from the data set for the following correlation results. Figure 5.7 and Figure 5.8 plot SUVA against four day TTHM concentration to determine the linear and second order polynomial R^2 coefficients, respectively.

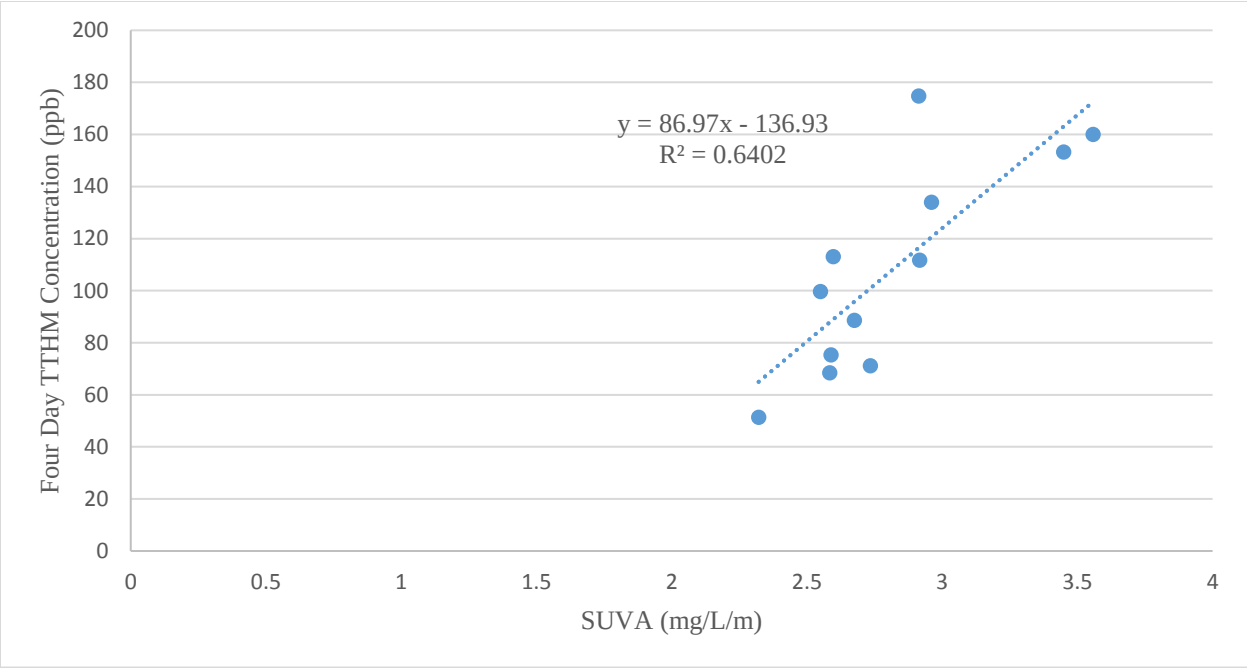

Figure 5.7: Linear Regression Correlation for SUVA to 4 day TTHM Content

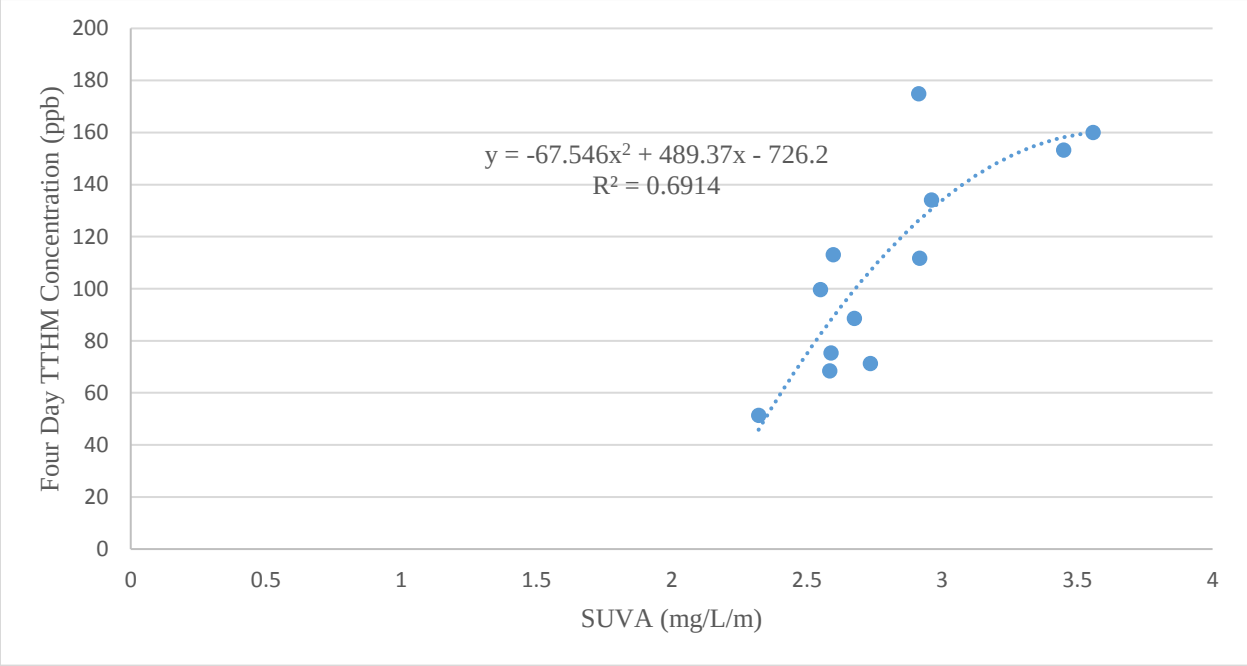

Figure 5.8: Polynomial Regression Correlation for SUVA to 4 day TTHM Content

The linear R^2 for SUVA was shown to be 0.640 while the second order polynomial regression revealed an improved R^2 of 0.691. These coefficients are significantly lower than those seen for both UV_{254} and DOC. These results reveal that for this data set, the relationship of aromaticity to four day TTHM content is not strong and reinforces the UV_{254} results which showed that high aromaticity impacts correlation results for this data set.

Fluorescence Spectroscopy Analysis

Fluorescence spectroscopy measures the fraction of DOM that is able to both absorb and emit light. The advantage of this technique over other organic analysis is the ability to characterize different DOM signatures based on peak absorbances associated with different types of organics. By emitting a range of emission wavelengths of light and measuring the absorbance at a range excitation wavelengths, a 3-D excitation- emission matrix (EEM) was formed for each sample. Different organic substances such as humic and fulvic acids are particular to specific combinations of the excitation and emission wavelengths such that peaks in the absorbance seen on the EEMs can indicate whether the organics are humic-like, fulvic-like, etc. in nature (Chen et al., 2003). Figure 5.9 presents a three dimensional EEM for the OLL well site representing the sample location with the highest four day TTHM concentration.

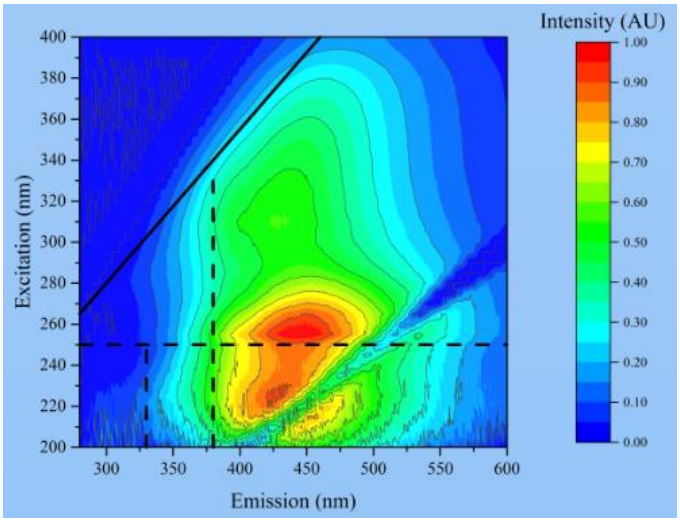

Figure 5.9: Three Dimensional EEM for OLL well

The fluorescence regional integration (FRI) method as outlined by Chen et al. (2003) was used to analyze the EEM data for the sample set. The EEM was divided into predetermined regions based on different types of organic fractions and the total volume under each region was determined and compared. The volume was determined by taking the emission-excitation area (nm^2) for each data point based on the bandwidth parameters chosen and multiplying it by the fluorescence intensity in arbitrary units (AU) at that point. The total volume for the humic and fulvic-like regions (V and III respectively) are presented in Table 5.4 for each of the analyzed samples. Data for the other regions is presented in further detail in Appendix C.

Table 5.4: FRI Regional Volumes for Humic and Fulvic acid-like Organic Fractions

Sample ID	Humic-like Regional Volume (AU-nm^2)	Fulvic-like Regional Volume (AU-nm^2)
JUP	$1.83 \cdot 10^8$	$3.64 \cdot 10^7$
OLL	$1.31 \cdot 10^8$	$6.31 \cdot 10^7$
V3	$1.26 \cdot 10^8$	$4.96 \cdot 10^7$
LG3	$1.24 \cdot 10^8$	$5.12 \cdot 10^7$
AH1	$9.72 \cdot 10^7$	$4.62 \cdot 10^7$
AMH	$8.56 \cdot 10^7$	$4.13 \cdot 10^7$
BP2	$8.47 \cdot 10^7$	$3.71 \cdot 10^7$
LG1	$6.50 \cdot 10^7$	$2.39 \cdot 10^7$
LG2	$5.81 \cdot 10^7$	$2.16 \cdot 10^7$
V2	$5.16 \cdot 10^7$	$1.60 \cdot 10^7$
V1	$4.14 \cdot 10^7$	$1.23 \cdot 10^7$
LR	$3.89 \cdot 10^7$	$1.57 \cdot 10^7$
AH2	$1.88 \cdot 10^7$	$4.63 \cdot 10^6$

Results show that the regional volume for humic-like substances ranged from $1.88 \cdot 10^7$ to $1.83 \cdot 10^8$ AU·nm^2 while the regional volume for fulvic-like substances ranged from $4.63 \cdot 10^6$ to $6.31 \cdot 10^7$ AU·nm^2. Although it appears as though the humic substances dominate the fulvic substances, this is due to the discrepancy in regional area as previously shown in Figure 2.3. To account for this discrepancy, regional volumes can be normalized to the total area to make regional volumes comparable between each other. This technique is utilized further in this section, however, the data presented in Table 5.4 can be used as shown to correlate the amount of humic and fulvic substances to TTHM concentration. Linear and second order polynomial regression correlation results are presented in Figure 5.10 and Figure 5.11Figure 5.12 for Region V (humic acid) and in Figure 5.12 and Figure 5.13 for Region III (fulvic acid).

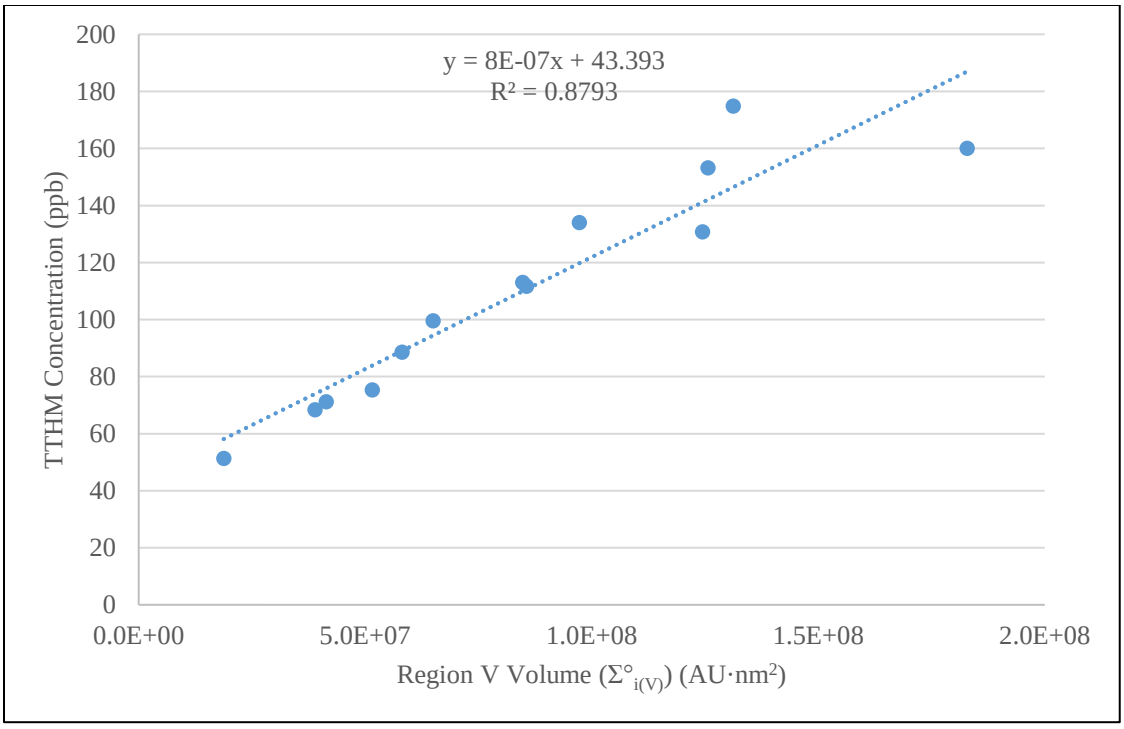

Figure 5.10 : Linear Regression Correlation for Region V and 4day TTHM Content

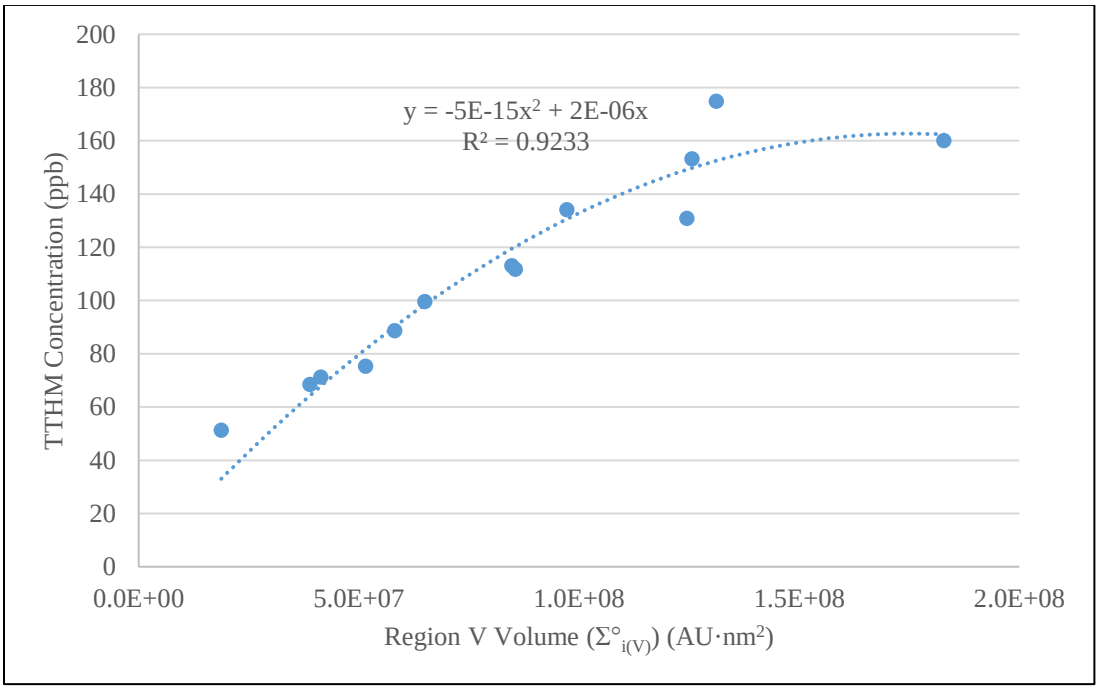

Figure 5.11: Polynomial Regression Correlation for Region V and 4 day TTHM Content

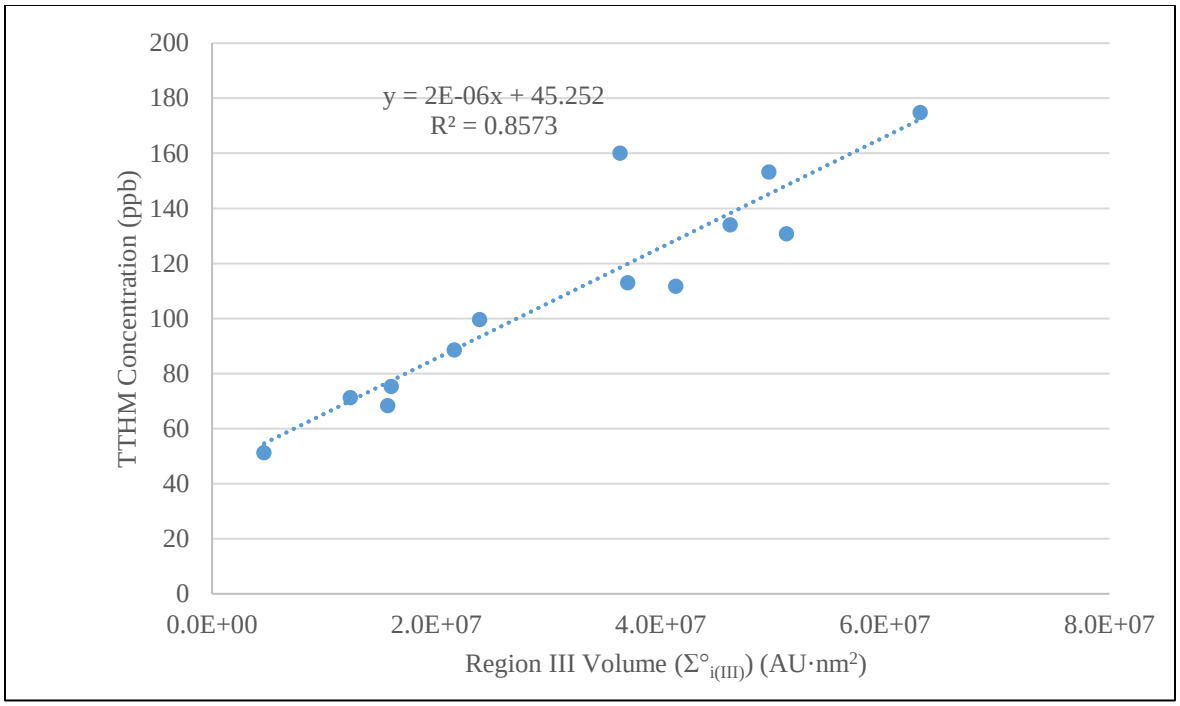

Figure 5.12 : Linear Regression Correlation for Region III and 4 day TTHM Content

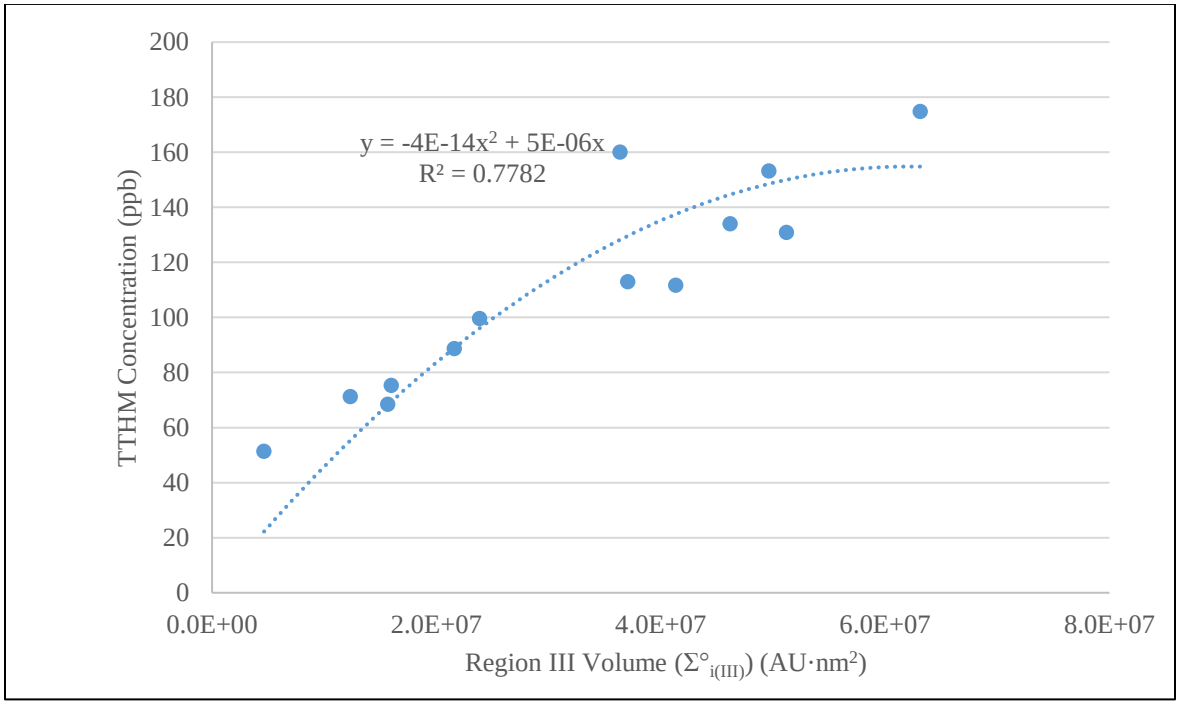

Figure 5.13: Polynomial Regression Correlation for Region III and 4 Day TTHM Content

The R^2 for the correlation between humic and fulvic substances and the four-day TTHM concentration are shown to be 0.879 and 0.857, respectively, for the linear regression and 0.92 and 0.78 respectively, for the polynomial regression. This shows the humic-like fraction of the organics have a higher correlation to four day TTHM concentration compared to the fulvic-like fraction for this data set. It is still shown, however, that both constituents of the organic composition have strong positive correlations with TTHM formation.

When comparing the contribution of the humic and fulvic fractions for each sample, it can be shown that the sample with the highest humic regional volume did not have the highest fulvic regional volume in the data set. This indicates that the humic and fulvic fractions of different source waters have different contributions towards the four day TTHM concentration can imply that a correlation of either individual region with four day TTHM concentration would be weaker than a correlation with the combined regional volumes. When the total volumes under both regions III and V are combined, the linear R^2 increased to 0.95 as is shown in Figure 5.14 while the polynomial R^2 increased to 0.91 from Figure 5.15.

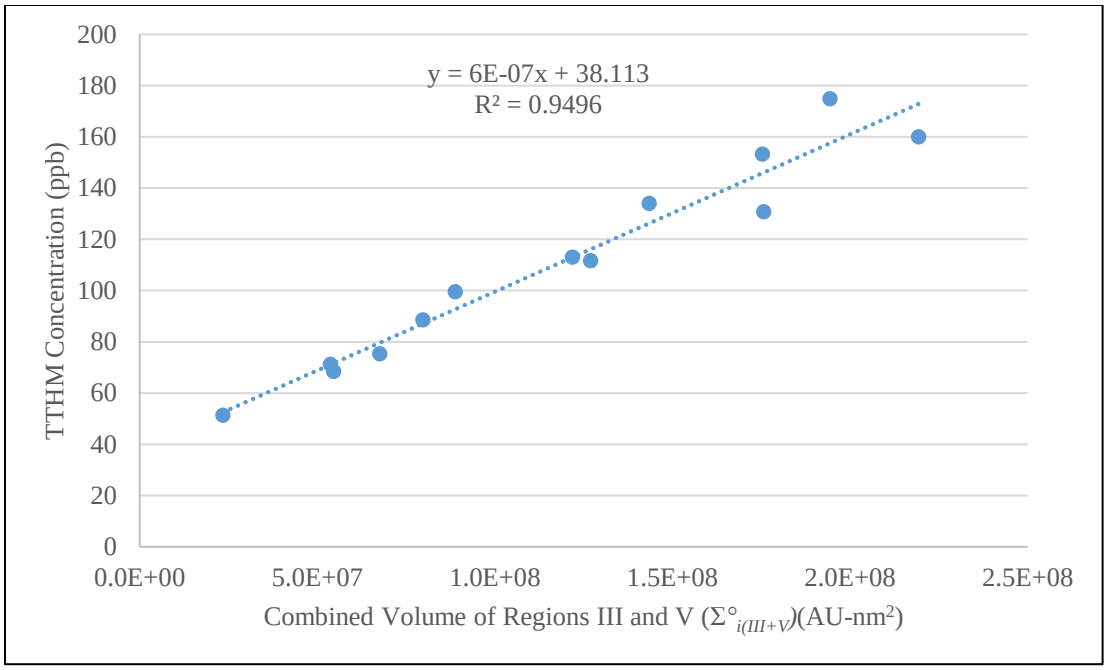

Figure 5.14 : Linear Regression Correlation for Region III + V to 4 day TTHM Content

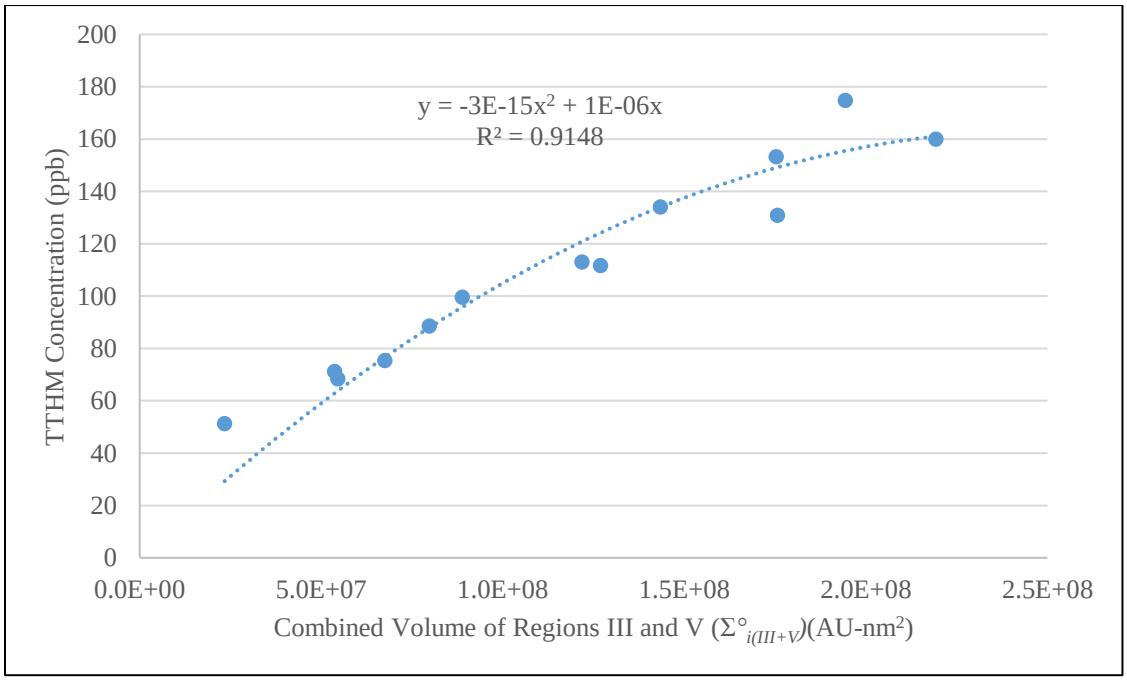

Figure 5.15: Polynomial Regression Correlation for Region III+V to 4 day TTHM Content

As previously mentioned, normalizing the volumes of each region to the total area allows regions to be internally comparable with each other. The normalization technique to an equalized set of areas as defined by Chen et al. (2003), allows for comparison between volumes under two different regions as well as for the percent composition of each of the different organic regions. Table 5.5 presents the normalized volumes for regions V and III (humic and fulvic-like respectively) while Table 5.6 presents the percentage contribution for regions V and III.

Table 5.5: FRI Normalized Volumes for Regions V and III

Sample ID	Region V Normalized Volume (AU-nm^2)	Region III Normalized Volume (AU-nm^2)
JUP	$3.07 \cdot 10^8$	$1.76 \cdot 10^8$
OLL	$2.20 \cdot 10^8$	$3.06 \cdot 10^8$
V3	$2.11 \cdot 10^8$	$2.40 \cdot 10^8$
LG3	$2.09 \cdot 10^8$	$2.48 \cdot 10^8$
AH1	$1.63 \cdot 10^8$	$2.24 \cdot 10^8$
AMH	$1.44 \cdot 10^8$	$2.00 \cdot 10^8$
BP2	$1.42 \cdot 10^8$	$1.79 \cdot 10^8$
LG1	$1.09 \cdot 10^8$	$1.15 \cdot 10^8$
LG2	$9.76 \cdot 10^7$	$1.05 \cdot 10^8$
V2	$8.66 \cdot 10^7$	$7.74 \cdot 10^7$
V1	$6.95 \cdot 10^7$	$5.97 \cdot 10^7$
LR	$6.53 \cdot 10^7$	$7.58 \cdot 10^7$
AH2	$3.15 \cdot 10^7$	$2.24 \cdot 10^7$

Table 5.6: Percentage Contribution for Regions V and III

Sample ID	Percentage Region V (%)	Percentage Region III (AU-nm^2)
JUP	41.5	23.8
OLL	26.0	36.0
V3	29.3	33.4
LG3	22.9	27.1
AH1	22.5	30.8
AMH	26.7	37.2
BP2	22.8	28.8

Sample ID	Percentage Region V (%)	Percentage Region III (AU-nm^2)
LG1	23.7	25.1
LG2	24.4	26.1
V2	28.7	25.7
V1	33.2	28.6
LR	29.9	34.7
AH2	34.9	24.8

Based on the normalized values, it is shown that some samples have a higher volume for fulvic fractions when compared to the humic fractions. This is shown in the Jupiter and OLL samples where the humic fraction dominates for Jupiter and the fulvic fraction dominates for OLL, even though both samples were shown to have high TTHM formation. This is a possible explanation for the combination of humic and fulvic volumes in Figure 5.14 and Figure 5.15 having higher coefficients of determination than that for the individual regional volume correlations. The normalized volume data can also be used to analyze the percent fractionations of each of the five regional organic constituents for each sample. Figure 5.16 illustrates the percent composition for each of the samples to show the aforementioned difference in region V (humic) and region III (fulvic) percentages.

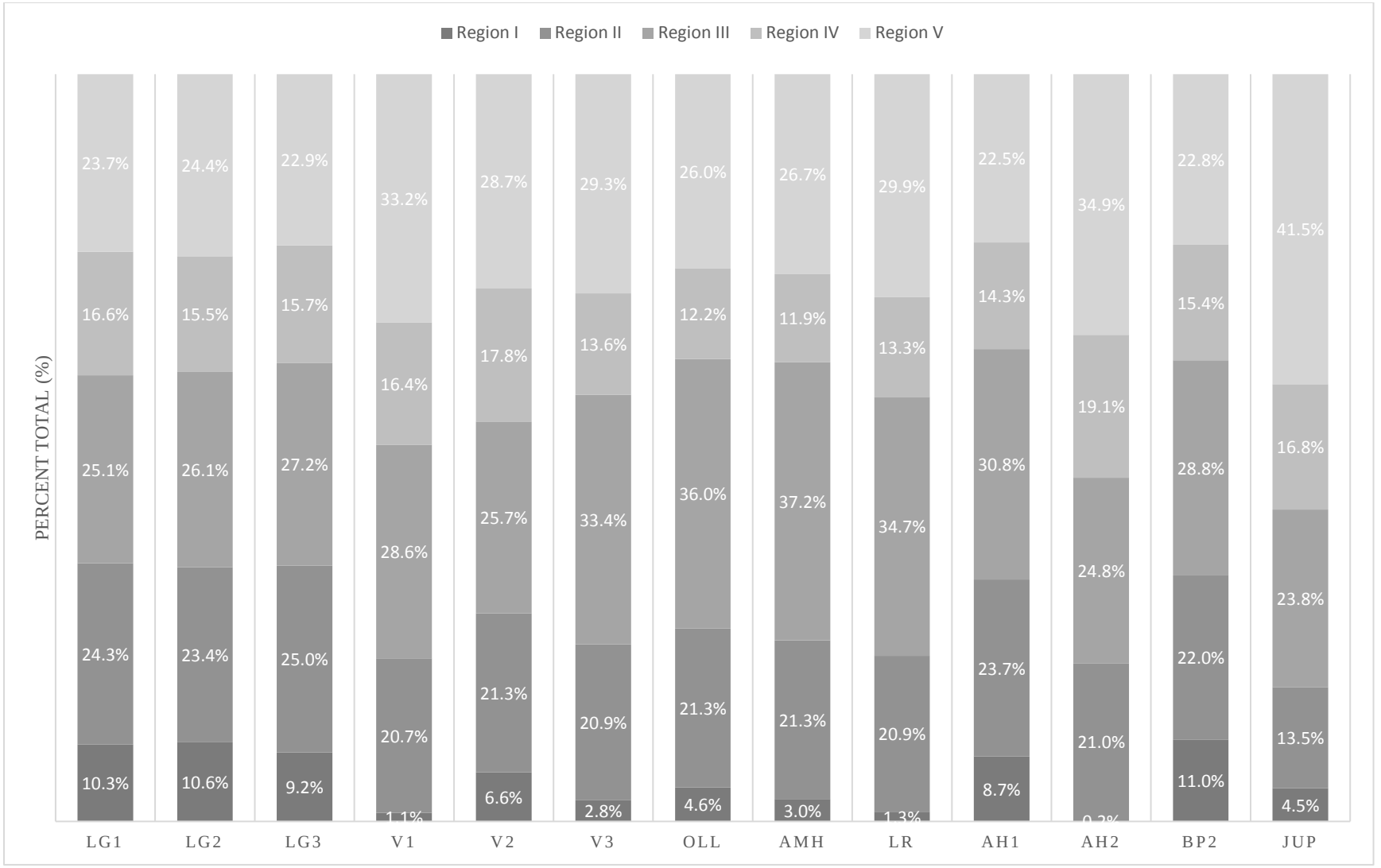

Figure 5.16: Regional Fractionation for each Sample

Application of this technique has been used to characterize the composition and transformation of organic material in areas such as landfill leachates (He et al., 2011) and membrane fouling in submerged membrane bioreactors (Wang et al., 2009). Although this technique is useful for an understanding of the change in composition of organics over time, plotting the percentage of humic and fulvic material against TTHM concentration revealed no statistically significant correlation between the percentages and TTHM formation potential as the coefficients of determination for these two correlations were both less than 0.100.

Modeling Results

Using the equations from each of the correlation regressions, the predicted four day TTHM concentrations were plotted against the actual values to determine which correlation had the strongest predicting capabilities. DOC and region III+V combined fluorescence were the strongest predictor variables based on this analysis. Table 5.7 presents the predicted four day TTHM values using the linear and polynomial regression equations for both DOC and region III+V fluorescence and compares the predicted values to the actual values. Figure 5.17 and Figure 5.18 plot the predicted TTHM values against the actual values.

Table 5.7: Predicted TTHM values for DOC and Region III+V Fluorescence Model

Sample ID	Actual TTHM (ppb)	DOC Linear Predicted TTHM (ppb)	DOC Polynomial Predicted TTHM (ppb)	Region III+V Linear Predicted TTHM (ppb)	Region III+V Polynomial Predicted TTHM (ppb)
JUP	160.1	168.8	166.3	169.8	160.3
OLL	174.8	168.8	166.3	154.6	154.8
V3	153.2	141.7	143.3	143.5	148.6
LG3	130.9	120.6	123.2	143.2	148.5
AH1	134	132.5	133.7	124.2	133.6
AMH	111.7	95.7	97.1	114.3	123.7
BP2	112.9	132.5	134.7	111.2	120.4
LG1	99.6	99.5	101.2	91.5	95.6
LG2	88.6	95.1	96.5	85.9	87.6
V2	75.3	78.9	78.0	78.7	76.5
V1	71.2	82.7	82.4	70.3	62.7
LR	68.4	67.0	63.8	70.9	63.7
AH2	51.3	48.6	40.6	52.2	29.2

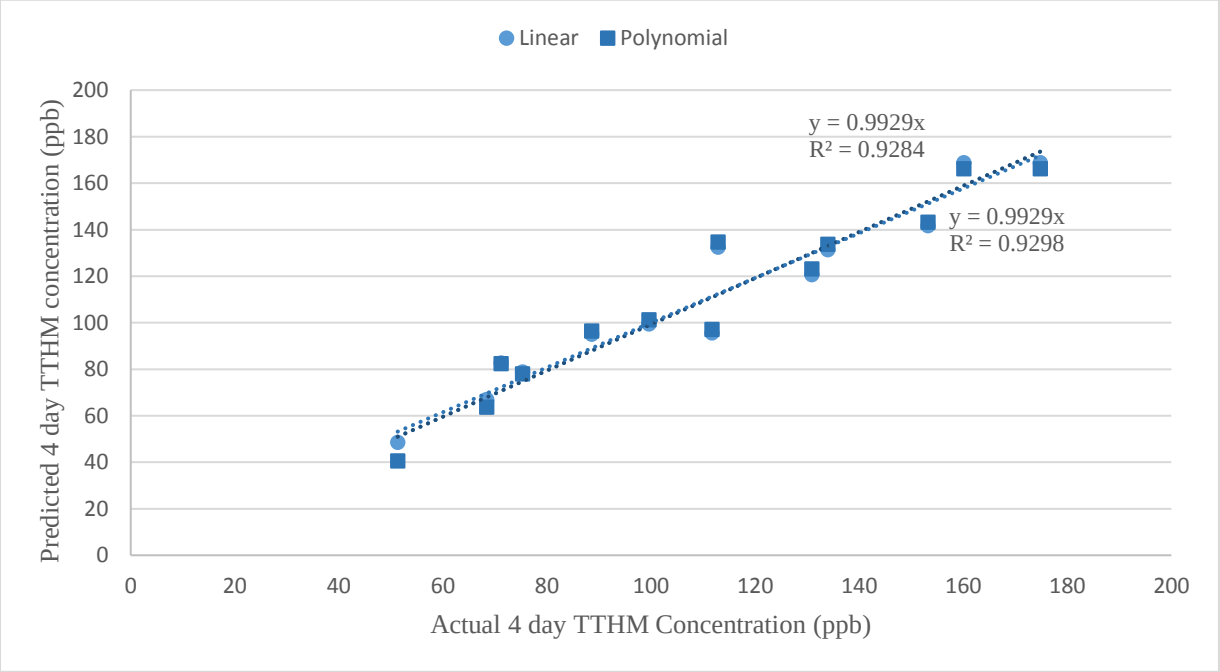

Figure 5.17: DOC Model for Actual Versus Predicted 4 day TTHM

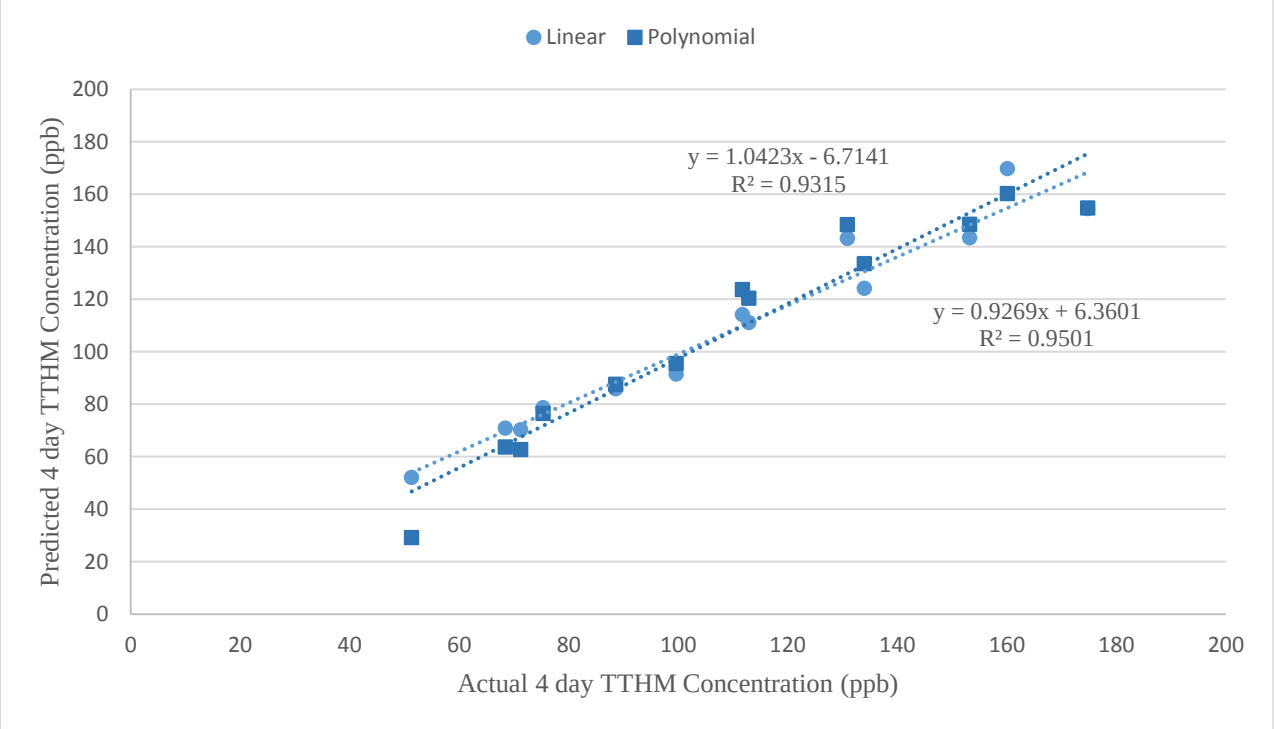

Figure 5.18: Region III+V Fluorescence Model for Actual Versus Predicted 4 day TTHM

Quality Control Results

An analysis for quality control was conducted to determine if the accuracy and precision of the experimental data set for TTHM, DOC, and UV_{254} results were within acceptable limits. Figure 5.19 presents a quality control chart based on percent recovery for accuracy for TTHMs while Figure 5.20, Figure 5.21, and Figure 5.22 present quality control charts based on the I-statistic value for precision for TTHM, DOC and UV_{254}, respectively. Results indicate that for the accuracy control chart, only two data points exceeded the LWL. The two data points in question were reanalyzed with acceptable results indicating that the original violation was most likely due to either human error or contamination. Results for the precision control chart indicate that one point exceeded the UCL for TTHM. This data point was excluded from the final results.

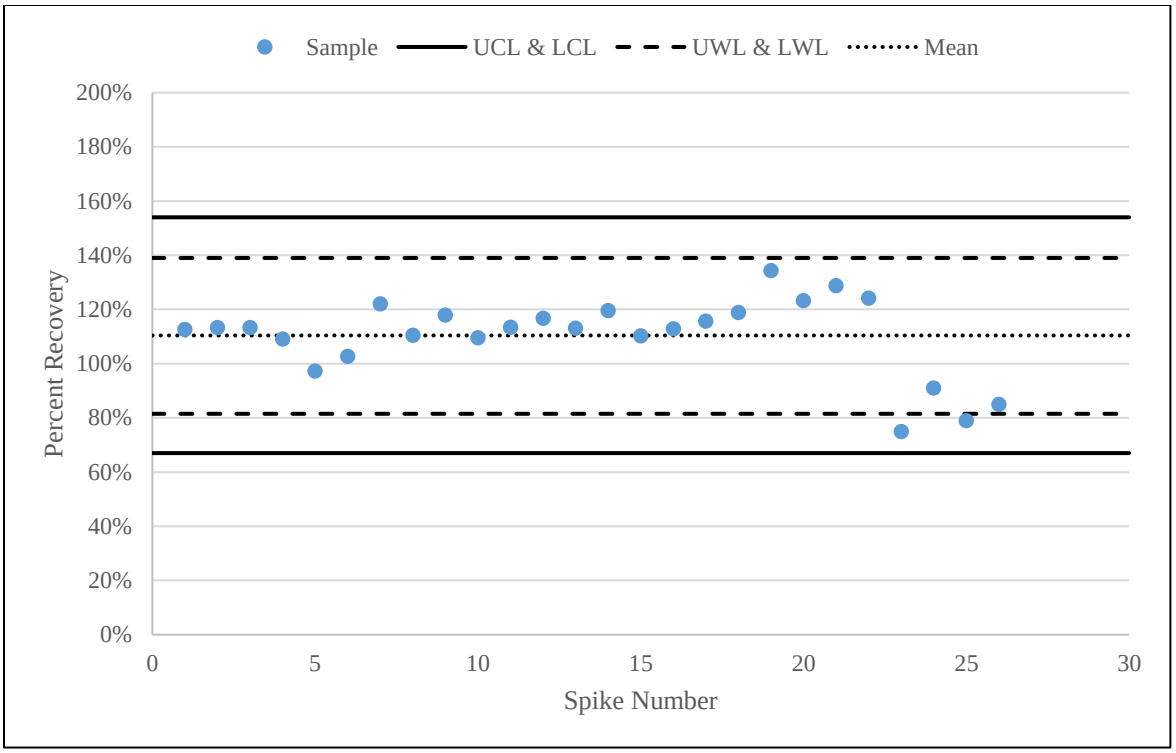

Figure 5.19 Control Chart for TTHM accuracy

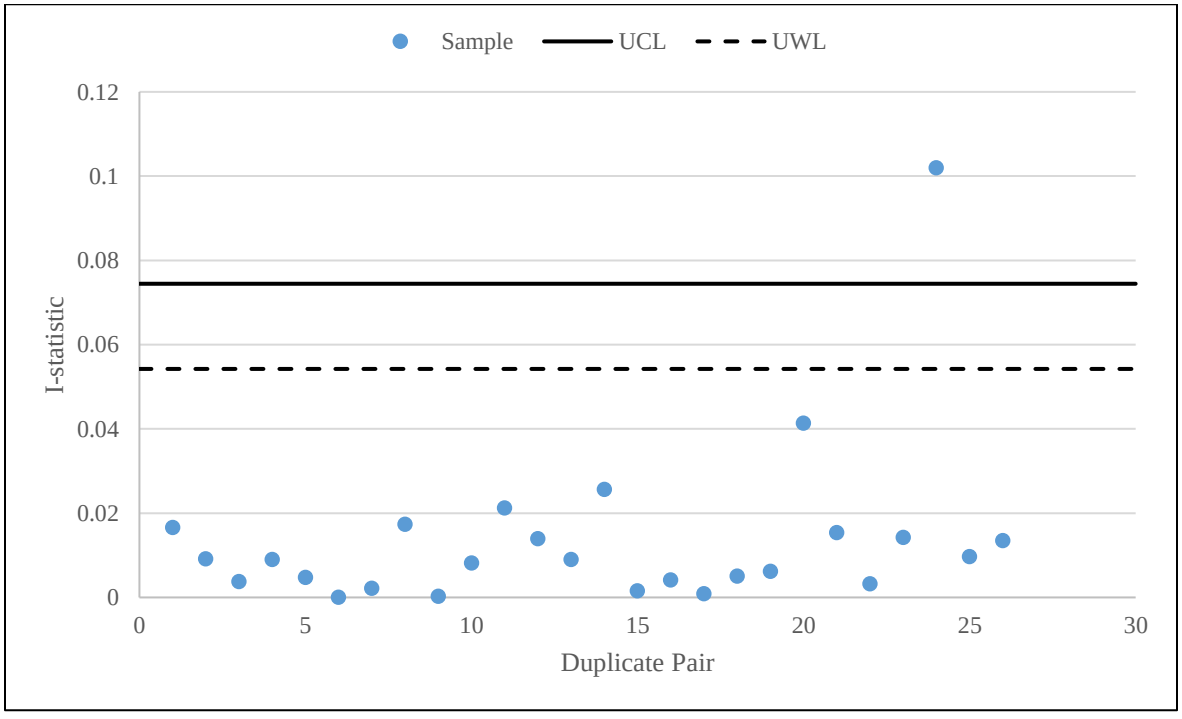

Figure 5.20 Control Chart for TTHM Precision

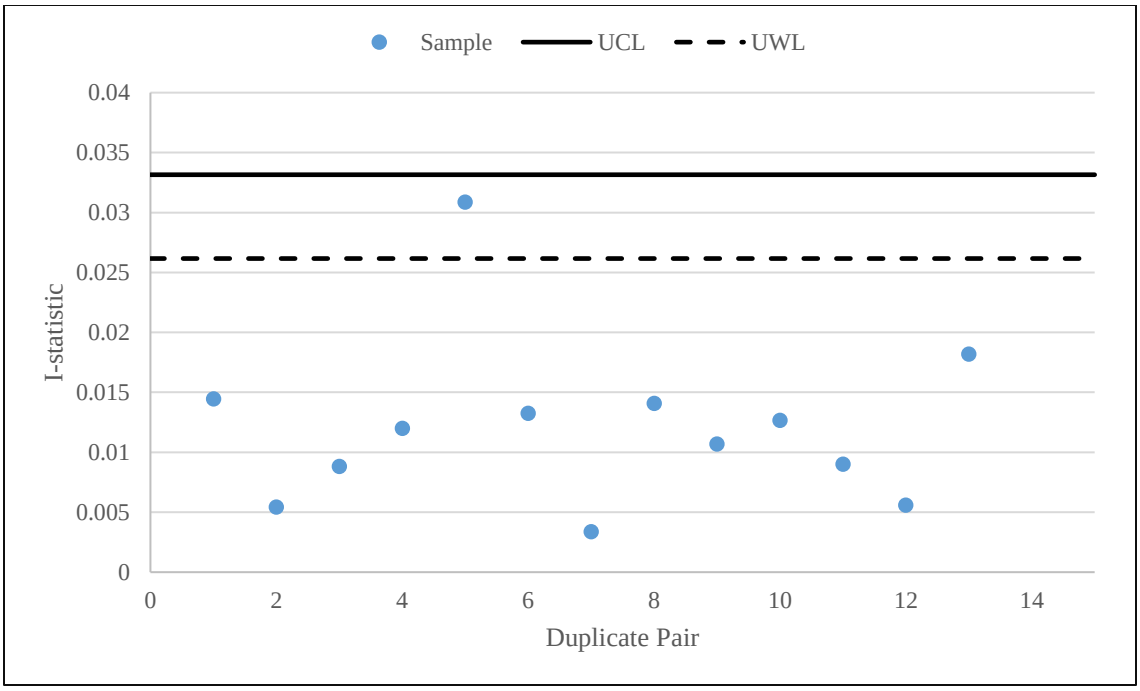

Figure 5.21: Control Chart for DOC Precision

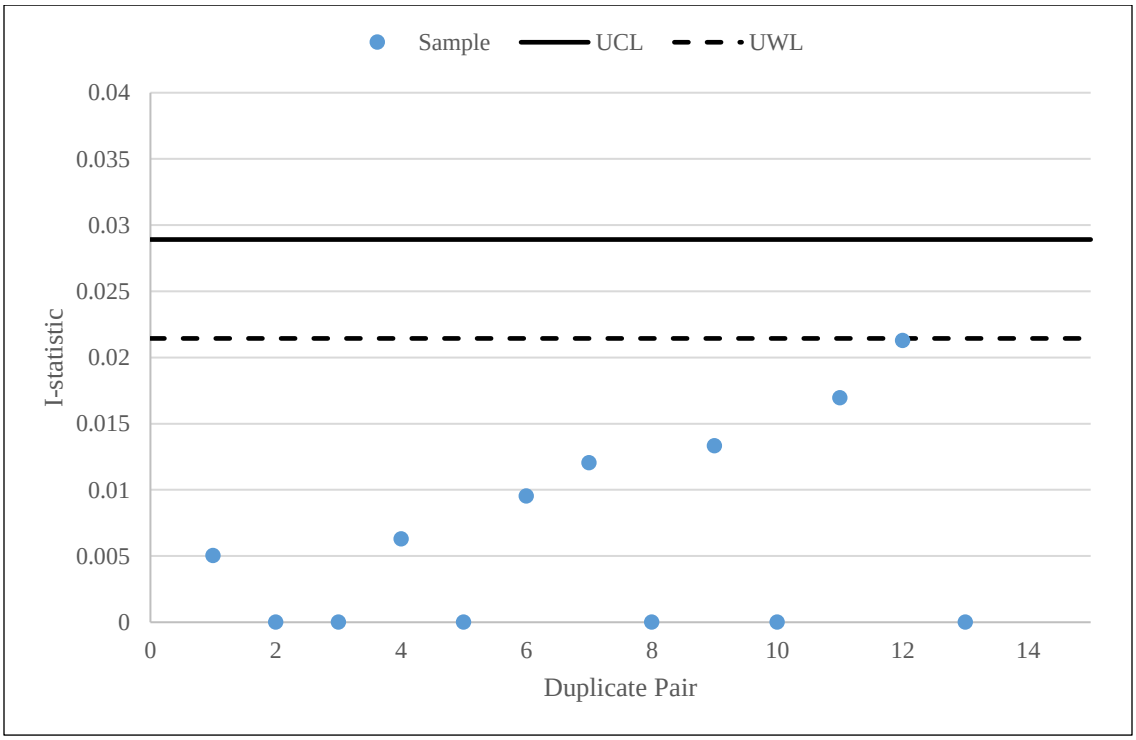

Figure 5.22: Control Chart for UV_{254} Precision

CHAPTER 6: CONCLUSIONS AND RECOMMENDATIONS

Conclusions

- Fluorescence and DOC were shown to have a strong linear correlation to four day simulated distribution system TTHM concentration when compared to UV_{254} and SUVA. Based on the results obtained through correlation studies, the combined integrated volume under regions III and V ($\Sigma°_{i(III+V)}$) obtained through fluorescence spectroscopy was shown to have the highest linear R^2 of 0.950. DOC showed to also have a high linear R^2 of 0.906 compared to the values of 0.836 and 0.640 for UV_{254} and SUVA respectively.
- A second order polynomial regression better represented the data for samples with high four day TTHM concentrations. Results revealed that using a second order polynomial regression produced a stronger correlation between DOC, UV_{254}, SUVA, and FRI for region V and four day TTHM content. The second order polynomial regression also produced a weaker correlation between FRI for region III, and FRI for regions III+V and four day TTHM content. The polynomial regression resulted in the strongest correlation between DOC and four day TTHM content with an R^2 of 0.937.
- For the FRI method, regions III and V produced a stronger correlation to four day simulated distribution system TTHM concentration than regions I, II, and IV. The coefficients of determination for the integrated volume under regions III and V were 0.857 and 0.880, respectively, compared to the R^2 values of 0.245, 0.623, and 0.743 for regions I, II, and IV, respectively. This reveals that the humic and fulvic fractions of NOM have stronger correlations to four day TTHM content than aromatic proteins or microbial like compounds.

- When correlating volumes of regions III and V to four day TTHM content, a stronger correlation was observed when the regional volumes were combined ($\Sigma°_{i(III+V)}$) as opposed to the individual regional volumes ($\Sigma°_{i(III)}$ and $\Sigma°_{i(V)}$). When the integrated volumes under regions III and V were combined, the coefficient of determination was observed to be 0.950 as compared to 0.857 and 0.880 for regions III and V, respectively. These results indicate that water sources are influenced by fulvic (region III) and humic (region V) fractions differently and that the combination of the two fractions increases the strength of the correlation to four day TTHM content.
- Fluorescence spectroscopy shows potential for predicting TTHM content in groundwaters. Other studies that have assessed the applicability of fluorescence for predicting TTHM formation in surface waters have had varying results, with the majority showing fluorescence to be a weaker surrogate parameter than DOC, UV_{254}, and SUVA. The results from this study indicated that FRI for regions III and V have a strong positive correlation (R^2 = 0.950 and 0.915 for linear and polynomial regressions respectively) with four day TTHM content in groundwaters. Further research would need to be conducted to conclude if fluorescence is a stronger surrogate to TTHM formation in groundwaters than in surface waters.
- Aromaticity was shown to impact the interpretation of UV_{254} and SUVA data when correlated with four day TTHM content. Results from the correlation between UV_{254} data and four day TTHM concentration revealed that samples with UV_{254} absorbance higher than 0.06 cm^{-1} had a weaker correlation with four day TTHM concentration, decreasing the R^2 from 0.932 to 0.836. These results imply the limitations of using UV_{254} as a surrogate

parameter of TTHM formation for source waters containing highly aromatic compounds. High aromaticity was also seen to impact SUVA results, which had the weakest correlation with four day TTHM concentration.

Recommendations

- Additional studies for samples containing very low and very high organics are recommended to determine if a polynomial regression is more appropriate for the data set. The range of the given data set showed primarily linear results, however, polynomial regressions could be better suited for the upper and lower ranges. More data points would be needed to determine if the second order polynomial regressions are stronger or weaker when the range of data is expanded.
- Additional studies to evaluate the alteration of NOM composition across treatment process trains for treated groundwaters are recommended. This study focused on two treatment processes commonly used for Florida groundwaters: aeration and chlorination. The composition and concentration of NOM has been shown to alter across traditional drinking water processes trains (Sohn et al., 2007) not simulated in this research. In order for the results to be applicable to different WTFs, further investigation using fluorescence spectroscopy to analyze the fate of fluorescing compounds across different treatment processes would need to be evaluated.
- Monitoring fluorescence, in conjunction with DOC and UV_{254}, for a water distribution system could aid water purveyors in projecting TTHM content in their system. Fluorescence data could be used to project DBP content changes in a water distribution system in the case where a system is altered or expanded through the inclusion of new

wellfields. It is recommended that water purveyors assess the feasibility of online fluorescence monitoring as the ability to correlate DBP formation in a drinking water distribution system to source water NPOC will assist in projecting TTHM content in the system.

- Additional studies with respect to specific components of the FEEM within each region should be conducted to further identify better correlation to TTHMs. For the groundwaters analyzed in this study, regions III and V showed the strongest correlations to TTHM content, however, other studies have shown that regions II and IV show stronger correlations for certain surface waters. This indicates that different water sources contain significantly varying organic compositions which can influence the formation of TTHMs differently. Further research into these difference are recommended to further assess the potential use of fluorescence monitoring in the drinking water industry.

APPENDIX A : WATER QUALITY DATA

Table A-1 Water Quality Results From In Field Testing

Well ID	Conductivity (µS/cm)	Temperature (°C)	pH	Turbidity (NTU)	True Color (PCU)	UV_{254} (cm^{-1})	Sulfides (mg/L)
LG1	517 ± 0	23.6 ± 0.2	7.50 ± 0.01	4.65 ± 0.35	< 5	0.038	BDL
LG2	482 ± 2	22.8 ± 0.2	7.48 ± 0.03	0.44 ± 0.04	< 5	0.038	0.16 ± 0.1
LG3	504 ± 1	24.7 ± 0.2	7.56 ± 0.02	0.21 ± 0.03	< 5	0.096	5.68 ± 0
V1	378 ± 1	23.1 ± 0.2	7.31 ± 0.04	0.21 ± 0.03	< 5	0.032	BDL*
V2	419 ± 1	22.7 ± 0.2	7.51 ± 0.01	0.33 ± 0.04	< 5	0.029	0.21 ± 0.1
V3	326 ± 0	23.1 ± 0.1	7.77 ± 0.05	0.71 ± 0.04	< 5	0.079	0.17 ± 0.1
OLL	313 ± 1	23.1 ± 0.1	8.08 ± 0.07	0.10 ± 0.02	< 5	0.081	0.2 ± 0.3
AMH	400 ± 1	23.1 ± 0.2	7.98 ± 0.04	0.12 ± 0.09	< 5	0.042	0.2 ± 0.2
LR	433 ± 1	23.2 ± 0.1	7.73 ± 0.01	0.09 ± 0.06	< 5	0.023	BDL*
AH1	208 ± 1	24.1 ± 0.4	8.33 ± 0.31	0.49 ± 0.03	< 5	0.061	0.14 ± 0
AH2	329 ± 0	23.8 ± 0.1	7.92 ± 0.02	0.26 ± 0.02	< 5	0.013	0.1 ± 0

Table A-2 Water Quality Results for In Lab Testing

Well ID	Calcium (mg/L)	Magnesium (mg/L)	Sodium (mg/L)	Iron (mg/L)	Chloride (mg/L)	Sulfate (mg/L)	Bromide (mg/L)	TDS (mg/L)	DOC (mg/L)
LG1	62.5	11.8	25.5	0.02	34	59	< 0.2	0.285	1.49
LG2	0.05	57.8	10.9	25.1	29	39	< 0.2	0.271	1.42
LG3	0.01	70.9	17.6	6.2	10	131	< 0.2	0.361	1.86
V1	46.2	10.9	10.9	0.01	22	28	< 0.2	0.190	1.17
V2	54.0	11.8	10.7	< 0.005	22	28	< 0.2	0.222	1.12
V3	40.0	12.2	6.9	0.03	14	13	< 0.2	0.168	2.29
OLL	45.0	8.7	5.2	0.03	12	8	< 0.2	0.220	2.78
AMH	54.6	12.2	8.0	0.04	18	32	< 0.2	0.157	1.44
LR	56.1	14.1	9.1	0.02	21	37	< 0.2	0.229	0.89
AH1	24.5	7.2	4.5	0.03	9	6	< 0.2	0.102	2.06
AH2	37.5	9.6	9.6	< 0.005	22	25	< 0.2	0.159	0.56

APPENDIX B : THM CONCENTRATION DATA

Table B-1: TTHM Time Series Concentration Data

Well ID	0.25 hour (ppb)	8 hour (ppb)	24 hour (ppb)	48 hour (ppb)	96 hour (ppb)
LG1	14.8	39.6	56.5	72.8	99.6
LG2	14.8	39.9	55.9	71.7	88.6
LG3	20.0	52.7	83.1	100.3	130.9
V1	14.6	40.0	55.4	65.9	71.2
V2	14.9	39.8	57.3	67.0	75.3
V3	27.3	72.6	111.1	138.5	153.2
OLL	30.9	86.6	134.1	151.1	174.8
AMH	16.1	53.0	76.7	93.9	111.7
LR	14.2	31.8	45.6	57.8	68.4
AH1	27.6	78.3	98.5	112.7	134.0
AH2	14.0	24.0	31.2	38.8	51.3
BP2	12.7	48.7	74.8	99.9	112.9
JUP	20.2	80.7	101.8	127	160.1

Table B-2: THM Time Series Concentration Data

Well ID	Hours After Dose (hr)	Chloroform (ppb)	Bromodichloromethane (ppb)	Dibromochloromethane (ppb)	Bromoform (ppb)
V1	0.25	< 10.0	1.6	< 1.0	< 2.0
	8	20.1	12.0	5.7	2.3
	24	21.5	10.3	3.9	2.0
	48	39.7	17.2	6.7	2.3
	96	42.3	14.9	5.3	2.1
V2	0.25	< 10.0	1.86	< 1.0	< 2.0
	8	16.8	12.3	7.7	3.0
	24	26.9	17.3	9.9	3.2
	48	34.9	19.0	10.0	3.1
	96	40.9	20.6	10.6	75.3
V3	0.25	21.7	2.6	< 1.0	< 2.0
	8	58.9	10.8	< 1.0	< 2.0
	24	91.8	16.2	1.1	< 2.0
	48	115.4	19.5	1.6	< 2.0
	96	129.6	20.0	1.6	< 2.0
LG1	0.25	< 10.0	1.8	< 1.0	< 2.0
	8	23.4	10.6	3.7	< 2.0
	24	35.8	14.1	4.5	< 2.0
	48	46.5	18.3	6.1	2.0
	96	66.4	23.5	7.5	2.1
LG2	0.25	< 10.0	1.8	< 1.0	< 2.0
	8	23.3	10.7	3.8	< 2.0
	24	34.0	14.7	5.2	< 2.0
	48	45.4	18.1	6.1	2.0
	96	57.2	21.9	7.5	2.1
AMH	0.25	< 10.0	3.1	< 1.0	< 2.0
	8	28.2	15.7	7.0	2.2
	24	42.6	22.1	9.5	2.4
	48	54.0	26.4	11.0	2.4
	96	68.1	29.6	11.5	2.4
LR	0.25	< 10.0	1.2	< 1.0	2.0
	8	10.4	9.4	8.2	3.8
	24	15.1	14.4	11.8	4.4
	48	22.2	18.0	13.3	4.4
	96	27.9	20.8	14.9	4.8
OLL	0.25	23.9	4.0	< 1.0	< 2.0
	8	67.9	15.3	1.5	< 2.0
	24	107.0	22.5	2.6	< 2.0
	48	122.9	23.7	2.6	< 2.0
	96	144.9	25.2	2.7	< 2.0
AH1	0.25	22.1	2.6	< 1.0	< 2.0
	8	62.7	12.6	1.0	< 2.0
	24	80.2	15.1	1.2	< 2.0
	48	92.6	16.8	1.3	< 2.0
	96	111.7	18.8	1.6	< 2.0

Well ID	Hours After Dose (hr)	Chloroform (ppb)	Bromodichloromethane (ppb)	Dibromochloromethane (ppb)	Bromoform (ppb)
AH2	0.25	< 10.0	< 1.0	< 1.0	< 2.0
	8	< 10.0	5.7	4.9	3.4
	24	< 10.0	9.3	7.8	4.0
	48	11.2	12.7	10.3	4.6
	96	15.8	17.3	13.1	5.2
LG3	0.25	14.9	2.1	< 1.0	< 2.0
	8	39.4	10.0	1.3	< 2.0
	24	63.3	15.4	2.4	< 2.0
	48	78.1	17.5	2.7	< 2.0
	96	104.0	21.4	3.4	< 2.0
JUP	0.25	17.2	< 1.0	< 1.0	< 1.0
	12	63.9	14.8	< 1.0	< 1.0
	24	81.3	18.5	< 1.0	< 1.0
	48	103.6	22.4	< 1.0	< 1.0
	72	120.6	25.5	< 1.0	< 1.0
	96	130.8	26.8	1.4	< 1.0
BP2	0.25	9.6	1.7	< 0.7	< 0.7
	12	41.3	16.0	5.8	< 0.7
	24	47.4	19.2	6.4	< 0.7
	48	68.6	23.3	7.3	< 0.7
	72	74.4	25.5	7.8	< 0.7
	96	96.4	27.9	8.4	< 0.7

APPENDIX C : FRI FLUORESCENCE DATA

Table C-1: FRI Fluorescence Data

Well ID	Region	Blank Corrected Regional Volume (AU·nm^2)*	Normalized Regional Volume (AU·nm^2)*	Regional Percent by Normalized Volume (%)
V1	I	1.12E+05	2.40E+06	1.15%
	II	2.02E+06	4.32E+07	20.69%
	III	1.23E+07	5.97E+07	28.56%
	IV	3.57E+06	3.42E+07	16.37%
	V	4.14E+07	6.95E+07	33.23%
V2	I	9.26E+05	1.98E+07	6.57%
	II	3.00E+06	6.42E+07	21.29%
	III	1.60E+07	7.74E+07	25.65%
	IV	5.60E+06	5.37E+07	17.80%
	V	5.16E+07	8.66E+07	28.69%
V3	I	9.51E+05	2.03E+07	2.83%
	II	7.01E+06	1.50E+08	20.85%
	III	4.96E+07	2.40E+08	33.39%
	IV	1.02E+07	9.78E+07	13.59%
	V	1.26E+08	2.11E+08	29.33%
LG1	I	2.21E+06	4.72E+07	10.28%
	II	5.21E+06	1.11E+08	24.27%
	III	2.39E+07	1.15E+08	25.14%
	IV	7.94E+06	7.61E+07	16.57%
	V	6.50E+07	1.09E+08	23.74%
LG2	I	1.98E+06	4.24E+07	10.59%
	II	4.38E+06	9.38E+07	23.43%
	III	2.16E+07	1.05E+08	26.12%
	IV	6.47E+06	6.20E+07	15.49%
	V	5.81E+07	9.76E+07	24.37%
AMH	I	7.54E+05	1.61E+07	3.00%
	II	5.35E+06	1.14E+08	21.25%
	III	4.13E+07	2.00E+08	37.19%
	IV	6.66E+06	6.39E+07	11.87%
	V	8.56E+07	1.44E+08	26.70%
LR	I	1.33E+05	2.85E+06	1.30%
	II	2.13E+06	4.56E+07	20.85%
	III	1.57E+07	7.58E+07	34.65%
	IV	3.04E+06	2.92E+07	13.33%
	V	3.89E+07	6.53E+07	29.86%
OLL	I	1.81E+06	3.88E+07	4.58%
	II	8.43E+06	1.80E+08	21.26%
	III	6.31E+07	3.06E+08	36.03%
	IV	1.07E+07	1.03E+08	12.15%
	V	1.31E+08	2.20E+08	25.97%
AH1	I	2.95E+06	6.31E+07	8.70%
	II	8.02E+06	1.72E+08	23.67%
	III	4.62E+07	2.24E+08	30.83%
	IV	1.08E+07	1.04E+08	14.28%
	V	9.72E+07	1.63E+08	22.51%

*Arbitrary Units (AU)

Well ID	Region	Blank Corrected Regional Volume (AU·nm^2)*	Normalized Regional Volume (AU·nm^2)*	Regional Percent by Normalized Volume (%)
AH2	I	9.70E+03	2.08E+05	0.23%
	II	8.85E+05	1.89E+07	20.95%
	III	4.63E+06	2.24E+07	24.81%
	IV	1.80E+06	1.73E+07	19.14%
	V	1.88E+07	3.15E+07	34.87%
LG3	I	3.94E+06	8.42E+07	9.23%
	II	1.07E+07	2.28E+08	25.01%
	III	5.12E+07	2.48E+08	27.15%
	IV	1.50E+07	1.43E+08	15.72%
	V	1.24E+08	2.09E+08	22.90%

*Arbitrary Units (AU)

REFERENCES

American Public Health, A., Eaton, A. D., American Water Works, A., & Water Environment, F. (2005). *Standard methods for the examination of water and wastewater*. Washington, D.C.: APHA-AWWA-WEF.

Amy, G., Bull, R., Craun, G. F., Pegram, R., Siddiqui, M., & Organization, W. H. (2000). Disinfectants and disinfectant by-products.

Ates, N., Kitis, M., & Yetis, U. (2007). Formation of chlorination by-products in waters with low SUVA—correlations with SUVA and differential UV spectroscopy. *Water Research, 41*(18), 4139-4148.

Baghoth, S. A., Sharma, S. K., & Amy, G. L. (2011). Tracking natural organic matter (NOM) in a drinking water treatment plant using fluorescence excitation–emission matrices and PARAFAC. *Water Research, 45*(2), 797-809. Bahram, M., Bro, R., Stedmon, C., & Afkhami, A. (2006). Handling of Rayleigh and Raman scatter for PARAFAC modeling of fluorescence data using interpolation. *Journal of Chemometrics, 20*(3-4), 99-105.

Bridgeman, J., Bieroza, M., & Baker, A. (2011). The application of fluorescence spectroscopy to organic matter characterisation in drinking water treatment. *Reviews in Environmental Science and Bio/Technology, 10*(3), 277.

Chen, W., Westerhoff, P., Leenheer, J. A., & Booksh, K. (2003). Fluorescence Excitation−Emission Matrix Regional Integration to Quantify Spectra for Dissolved Organic Matter. *Environmental Science & Technology, 37*(24), 5701-5710.

Coble, P. G. (1996). Characterization of marine and terrestrial DOM in seawater using excitation-emission matrix spectroscopy. *Marine Chemistry, 51*(4), 325-346.

Duranceau, S., & Jeffery, S. (2013). *Impact of Temperature and Bromide on Total Trihalomethane Formation in Membrane Permeate Blends.* Paper presented at the Proc. 2013 Florida Section AWWA Fall Conf., Champions Gate, Fla.

Hall, G. J., & Kenny, J. E. (2007). Estuarine water classification using EEM spectroscopy and PARAFAC–SIMCA. *Analytica Chimica Acta, 581*(1), 118-124. He, X.-S., Xi, B.-D., Wei, Z.-M., Jiang, Y.-H., Yang, Y., An, D., . . . Liu, H.-L. (2011). Fluorescence excitation–emission matrix spectroscopy with regional integration analysis for characterizing composition and transformation of dissolved organic matter in landfill leachates. *Journal of Hazardous Materials, 190*(1–3), 293-299. Hickenbottom, K. L., Hancock, N. T., Hutchings, N. R., Appleton, E. W., Beaudry, E. G., Xu, P., & Cath, T. Y. (2013). Forward osmosis treatment of drilling mud and fracturing wastewater from oil and gas operations. *Desalination, 312*, 60-66.

Hua, G., Reckhow, D. A., & Abusallout, I. (2015). Correlation between SUVA and DBP formation during chlorination and chloramination of NOM fractions from different sources. *Chemosphere, 130*, 82-89.

Johnstone, D. W., & Miller, C. M. (2009). Fluorescence excitation–emission matrix regional transformation and chlorine consumption to predict trihalomethane and haloacetic acid formation. *Environmental engineering science, 26*(7), 1163-1170.

Jung, C.-W., & Son, H.-J. (2008). The relationship between disinfection by-products formation and characteristics of natural organic matter in raw water. *Korean Journal of Chemical Engineering*, *25*(4), 714-720.

Korak, J. A., Dotson, A. D., Summers, R. S., & Rosario-Ortiz, F. L. (2014). Critical analysis of commonly used fluorescence metrics to characterize dissolved organic matter. *Water Research, 49*, 327-338.

Krasner, S. W., McGuire, M. J., Jacangelo, J. G., Patania, N. L., Reagan, K. M., & Aieta, E. M. (1989). The Occurrence of Disinfection By-products in US Drinking Water. *Journal (American Water Works Association), 81*(8), 41-53.

Lawaetz, A. J., & Stedmon, C. A. (2009). Fluorescence intensity calibration using the Raman scatter peak of water. *Applied spectroscopy, 63*(8), 936-940.

Murphy, K. R., Stedmon, C. A., Graeber, D., & Bro, R. (2013). Fluorescence spectroscopy and multi-way techniques. PARAFAC. *Analytical Methods, 5*(23), 6557-6566.

Peiris, R. H., Hallé, C., Budman, H., Moresoli, C., Peldszus, S., Huck, P. M., & Legge, R. L. (2010). Identifying fouling events in a membrane-based drinking water treatment process using principal component analysis of fluorescence excitation-emission matrices. *Water Research, 44*(1), 185-194.

Peleato, N. M., & Andrews, R. C. (2015). Comparison of three-dimensional fluorescence analysis methods for predicting formation of trihalomethanes and haloacetic acids. *Journal of Environmental Sciences, 27*, 159-167.

Pifer, A. D., & Fairey, J. L. (2014). Suitability of organic matter surrogates to predict trihalomethane formation in drinking water sources. *Environmental engineering science, 31*(3), 117-126.

Richardson, S. (2005). New disinfection by-product issues: emerging DBPs and alternative routes of exposure. *Global Nest J, 7*(1), 43-60.

Rinnan, Å., Booksh, K. S., & Bro, R. (2005). First order Rayleigh scatter as a separate component in the decomposition of fluorescence landscapes. *Analytica Chimica Acta, 537*(1–2), 349-358. Rook, J. J. (1974). Formation of haloforms during chlorination of natural waters. *Water Treat. Exam., 23*, 234-243.

Singer, P. C. (1999). Humic Substances as Precursors for Potentially Harmful Disinfection By-Products. *Water Science and Technology, 40*(9), 25-30.

Sohn, J., Amy, G., & Yoon, Y. (2007). Process-train profiles of NOM through a drinking water treatment plant. *Journal (American Water Works Association), 99*(6), 145-153.

Stedmon, C., & Bro, R. (2008). Characterizing dissolved organic matter fluorescence with parallel factor analysis: a tutorial. *Limnology and Oceanography: Methods, 6*(11), 572-579.

Stedmon, C. A., Markager, S., & Bro, R. (2003). Tracing dissolved organic matter in aquatic environments using a new approach to fluorescence spectroscopy. *Marine Chemistry, 82*(3–4), 239-254. USEPA. (1979). Control of Trihalomehtanes in Drinking Water. Final Rule. *Federal Register, 44:68624*.

USEPA. (1998). National Primary Drinking Water Regulations: Disinfectants and Disinfection Byproducts. Final Rule. . *Federal Register, 63 FR 69390*, 69390-69476.

USEPA. (2006). National Primary Drinking Water Regulation : Stage 2 Disinfectant / Disinfection Byproducts. Final Rule. *Federal Register, 71 FR 387*, 387 - 493.

Wallace, B., Purcell, M., & Furlong, J. (2002). Total organic carbon analysis as a precursor to disinfection byproducts in potable water: Oxidation technique considerations. *Journal of Environmental Monitoring, 4*(1), 35-42.

Wang, Z., Wu, Z., & Tang, S. (2009). Characterization of dissolved organic matter in a submerged membrane bioreactor by using three-dimensional excitation and emission matrix fluorescence spectroscopy. *Water Research, 43*(6), 1533-1540. Weishaar, J. L., Aiken, G. R., Bergamaschi, B. A., Fram, M. S., Fujii, R., & Mopper, K. (2003). Evaluation of Specific Ultraviolet Absorbance as an Indicator of the Chemical Composition and Reactivity of Dissolved Organic Carbon. *Environmental Science & Technology, 37*(20), 4702-4708.

Yang, X., Shang, C., Lee, W., Westerhoff, P., & Fan, C. (2008). Correlations between organic matter properties and DBP formation during chloramination. *Water Research, 42*(8–9), 2329-2339.

Zhang, X.-l., Yang, H.-w., Wang, X.-m., Fu, J., & Xie, Y. F. (2013). Formation of disinfection by-products: Effect of temperature and kinetic modeling. *Chemosphere, 90*(2), 634-639.